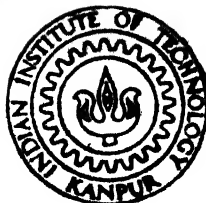


COORDINATION OF P.S.S. AND S.V.C. STABILIZERS BASED ON ROBUSTNESS CONSIDERATION

by

L. N. SHARMA

EE
1991
M
SHA
COO



DEPARTMENT OF ELECTRICAL ENGINEERING
INDIAN INSTITUTE OF TECHNOLOGY KANPUR

JULY, 1991

COORDINATION OF P.S.S. AND S.V.C. STABILIZERS BASED ON ROBUSTNESS CONSIDERATION

*A Thesis Submitted
in Partial Fulfilment of the Requirements
for the Degree of
MASTER OF TECHNOLOGY*

by
L. N. SHARMA

to the
DEPARTMENT OF ELECTRICAL ENGINEERING
INDIAN INSTITUTE OF TECHNOLOGY KANPUR
JULY, 1991

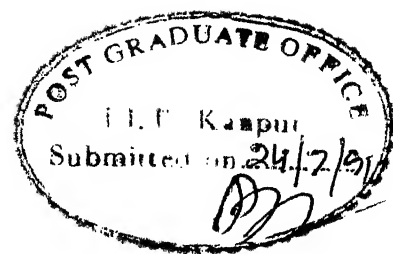
2 10/1991

112219

EE-1991-M-SHA-COO

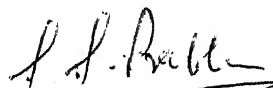
DEDICATED TO

KARNATAKA POWER CORPORATION



CERTIFICATE

It is certified that the work contained in the thesis entitled, "Coordination of P.S.S. and S.V.C. Stabilizers Based on Robustness Consideration" by Laxminarayana Sharma. A. has been carried out under my supervision and that this work has not been submitted elsewhere for a degree.


(S.S. Prabhu)
Professor

Department of Electrical Engineering
Indian Institute of Technology Kanpur

July, 1991

ACKNOWLEDGEMENTS

I could have this opportunity of doing my M.Tech. course at I.I.T. Kanpur, a premier Institute of our country only because of the genuine interest shown by Sri B. Vishwanath, Chief Engineer (Electrical), Varahi Hydroelectric Project, Karnataka and the management of Karnataka Power Corporation Ltd. in deputing me. I am grateful to them.

My present thesis is a brain-child of my teacher Dr. S.S. Prabhu. He gave me ideas, enough academic freedom and guided me whenever I was at cross road. I am grateful to him.

I am thankful to my teachers Dr. L.P. Singh, Dr. R.Arora, Dr. P.K. Kalra, Dr. S.C. Srivastava and Dr. R.K. Verma who taught me various courses and have given me encouragement at various stages during my stay at I.I.T. Kanpur.

I thank my classmates M/S. Krishna Patil, K. Raja Gopal, Manoj Kumar Agarwal and Nilesh Hiremath for their excellent company and help during my stay here.

My parents are great source of inspiration to me in life. I gratefully acknowledge their support.

Finally I am thankful to my wife for her patience and sincere cooperation.

L.N. SHARMA

CONTENTS

	PAGE
ABSTRACT	
LIST OF PRINCIPAL SYMBOLS	
LIST OF FIGURES	
LIST OF TABLES	
 CHAPTER 1 INTRODUCTION	 1
1.1 General	1
1.2 Effects of Thyristor Type Excitation System on Dynamic Stability	2
1.3 Methods of Damping Low Frequency Oscillations	3
1.4 Objectives and Scope of this Thesis	4
1.5 Review of Literature	4
1.6 Location of S.V.C.	6
1.7 Identifying Appropriate Signals	6
1.8 Summary of the Work Reported in this Thesis	7
 CHAPTER 2 SYSTEM MODELLING	 9
2.1 Introduction	9
2.2 Development of System Model	10
2.2.1 Generator Model	10
2.2.2 Excitation System Model	12
2.2.3 Static VAR Compensator	13
2.2.4 Linearized Model	16
2.2.5 Development of Output Equations	17
2.2.5.1 Output Equation Corresponding to PSS Input Signal	17
2.2.5.2 Output Equation Corresponding to SVC Stabilizer Input Signal	19
2.3 Numerical Example	20
2.4 Concluding Remarks	23
 CHAPTER 3 DESIGN OF STABILIZERS	 24
3.1 Introduction	24
3.2 Problem Formulation	24
3.3 Design Technique	26
3.4 Sector Criterion for Determining Robustness	28
3.5 Design and Coordination Methodology	28
3.5.1 PSS Design	30
3.5.2 SVC Design	31
3.5.3 Coordination of PSS and SVC Stabilizer	32

	PAGE
3.6 Choice of Closed Loop Eigenvalues	32
3.7 Numerical Results	33
3.7.1 Results with PSS	33
3.7.1.1 PSS with Generator Active Power Deviation ΔP_e as Input	33
3.7.1.2 PSS with Angular Velocity Deviation $\Delta\omega$ as Input	34
3.7.2 Results with SVC Stabilizer	34
3.7.2.1 SVC Stabilizer with Midline Active Power Deviation ΔP_m as Input	34
3.7.2.2 SVC Stabilizer With SVC Bus Angular Frequency Deviation $\Delta\omega_s$ As Input	35
3.7.3 Numerical Results with Both PSS and SVC Stabilizer Coordinated	35
3.7.3.1 ΔP_e Input PSS and ΔP_m Input SVC Stabilizer	36
3.7.3.2 $\Delta\omega$ Input PSS and $\Delta\omega_s$ Input SVC Stabilizer	36
3.7.3.3 ΔP_e Input PSS and $\Delta\omega_s$ Input SVC Stabilizer	36
3.7.3.4 $\Delta\omega$ Input PSS and ΔP_m Input SVC Stabilizer	37
3.8 A Few Remarks on Design	66
3.9 Concluding Remarks	67
CHAPTER 4 CONCLUSIONS	68
REFERENCES	70
APPENDIX A STATE SPACE MODEL OF THE SYSTEM	73
A.1 Development of the Model	73
A.1.1 Generator Model	73
A.1.2 Excitation System Model	74
A.1.3 S.V.C. Model	75
A.1.4 Linearized Model	75
A.1.4.1 Expression for ΔI_d and ΔI_q	75
A.1.4.2 Expression for ΔT_e	79
A.1.4.3 Expression for ΔV_t	79
A.1.4.4 Expression for ΔV_m	80

	PAGE
A.1.5 Output Equations	83
A.1.5.1 Output Equations Corresponding to PSS Signals	83
A.1.5.2 Output Equations Corresponding to SVC Stabilizer Signals	84
 APPENDIX B POWER SYSTEM DATA	 89
APPENDIX C POLE ASSIGNMENT WITH OUTPUT FEEDBACK	90

LIST OF TABLES

Table No.	Contents	Page
3.1	Numerical Results for ΔP_e Input PSS	38
3.2	Numerical Results for $\Delta \omega$ Input PSS	39
3.3	Numerical Results for ΔP_m Input SVC Stabilizer	40
3.4	Numerical Results for $\Delta \omega_s$ Input SVC Stabilizer	41
3.5	Numerical Results for Coordinated ΔP_e Input PSS and ΔP_m Input SVC Stabilizer	42
3.6	Numerical Results for Other Pairs of PSS (ΔP_e input) and SVC Stabilizer (ΔP_m input) not Selected for Coordination	45
3.7	Numerical Results for Coordinated $\Delta \omega$ Input PSS and $\Delta \omega_s$ Input SVC Stabilizer	48
3.8	Numerical Results for Other Pairs of PSS ($\Delta \omega$ Input) and SVC Stabilizer ($\Delta \omega_s$ input) not Selected for Coordination	51
3.9	Numerical Results for Coordinated ΔP_e Input PSS and $\Delta \omega_s$ Input SVC Stabilizer	54

LIST OF FIGURES

Fig. No.	Title	Page
2.1	Single-Machine Infinite-bus System with S.V.C.	11
2.2	IEEE Type-IS Excitation System	11
2.3	SVC Configurations	14
2.4	General Control Scheme of SVC	15
2.5	Block Diagram Representation of SVC Voltage Controller	15
2.6	Example System	22
3.1	Structure of P.S.S.	25
3.2	Structure of SVC Stabilizer	25
3.3	Sector Indicating the Permissible Location of Closed Loop Eigenvalues	29
3.4	Region of Robustness for ΔP_e Input PSS and ΔP_m Input SVC Stabilizer	43
3.5	Initial Condition Response of $\Delta\delta$; ΔP_e Input PSS, ΔP_m Input SVC Stabilizer	44
3.6	Region of Robustness for ΔP_e Input PSS and ΔP_m Input SVC Stabilizer not Selected for Coordination	46
3.7	Region of Robustness for $\Delta\omega$ Input PSS and $\Delta\omega_s$ Input SVC Stabilizer	49
3.8	Initial Condition Response of $\Delta\delta$; $\Delta\omega$ Input PSS, $\Delta\omega_s$ Input SVC Stabilizer	50
3.9	Region of Robustness for $\Delta\omega$ Input PSS and $\Delta\omega_s$ Input SVC Stabilizer not Selected for Coordination	52

		Page
3.10	Region of Robustness for ΔP_e Input PSS and $\Delta \omega_s$ Input SVC Stabilizer	55
3.11	Initial Condition Response of $\Delta \delta$; ΔP_e Input PSS, $\Delta \omega_s$ Input SVC Stabilizer	56
3.12	Region of Robustness for ΔP_e Input PSS and $\Delta \omega_s$ Input SVC Stabilizer not Selected for Coordination	58
3.13	Region of Robustness for $\Delta \omega$ Input PSS and PSS and ΔP_m Input SVC Stabilizer	61
3.14	Initial Condition Response of $\Delta \delta$; $\Delta \omega$ Input PSS and ΔP_m Input SVC Stabilizer	62
3.15	Region of Robustness for ΔP_e Input PSS and ΔP_m Input SVC Stabilizer not Selected for Coordination	64
A.1	Equivalent Circuit of the System	76

LIST OF PRINCIPAL SYMBOLS

p	Differential operator d/dt
Δ	Prefix to denote small changes about the operating point
o	Subscript to denote the value of the operating point
t	Time in seconds
ω_o	Synchronous angular velocity in radians per second
ω	Instantaneous angular velocity of rotor in radians per second
ω_s	Angular frequency of SVC bus in radians per second
δ	Rotor angle with respect to system reference in radians
V_∞	Infinite bus voltage magnitude in p.u.
V_t	Generator terminal voltage magnitude in p.u.
V_m	Transmission line midpoint voltage
V_d, V_q	d and q axes components of V_t
V_{md}, V_{mq}	d and q axes components of V_m
I_d, I_q	d and q axes component of stator current
X_d, X_q	d and q axes synchronous reactances
X_d'	d axes transient reactance
T_{do}	d axis transient open circuit time constant
H	Inertia constant in seconds
M	$\frac{2H}{\omega_o}$
K_D	Damping coefficient
E_{FD}	Generator field voltage in p.u.
P_e	Generator electrical power output in p.u.
T_e	Electrical torque developed
T_m	Mechanical torque input

R	Half line resistance
X	Half line reactance
B	SVC suceptance
K _A	Exciter voltage regulator gain
T _A	Exciter voltage regulator time constant
K _B	SVC voltage regulator gain
T _B	SVC voltage regulator time constant

ABSTRACT

This thesis demonstrates the significant benefits in the dynamic stability improvement of a power system, consisting of a synchronous generator connected to an infinite bus through a transmission line, by reactive power modulation at the generator terminal and at the mid-point of the transmission line, simultaneously. Reactive power modulation at the generator terminal is achieved by incorporating power system stabilizers while at the mid point of the transmission line it is achieved by means of Static Var compensator having an auxiliary controller. This thesis proposes a method to design and coordinate P.S.S. and S.V.C. stabilizer. The benefit derived in the robustness by such coordinated application of PSS and SVC is also demonstrated.

A suitable model for dynamic stability analysis of a single machine connected to the infinite bus through a transmission line with Static Var compensator at the mid point of the transmission line is also proposed.

The procedure followed here is simple. A set of P.S.S. is designed assuming that S.V.C. is not having an auxiliary controller. Similarly a set of S.V.C. stabilizer is designed

assuming that PSS is not connected in the system. The design point chosen is the same for both designs. The PSS and SVC stabilizer so designed are then coordinated so that when both are connected in the system a further improvement in the region of robustness is obtained. Pole placement technique is used for the stabilizer design and a sector criterion for eigenvalues is used for robustness.

The proposed method has been tested for various combinations of control signals.

CHAPTER 1

INTRODUCTION

1.1 General

Power system engineers have to operate their systems in such a way that they can meet the load demand on it in the most economical manner, ensure good quality and high reliability supply and meet various contingencies in operation effectively. This is a difficult task. It has been compounded by the fact that power systems have grown rapidly and have become very complex, to meet with the ever increasing load demand.

Enhancement of power system stability is a major factor in improving the reliability and quality of the system. Power system engineers speak of three types of stability. The first is steady state stability which puts a limit on the maximum power transfer capability of the system. The second is transient stability. It is the capacity of the system to withstand major shocks like loss of a generating unit, loss of a major transmission line or a severe network fault without losing synchronism. And the third is dynamic stability. We confine ourselves in this thesis to the problem of dynamic stability.

In a power system small magnitude random changes in load take place at all times, with the accompanying adjustment of generation. When load on the system changes, the generators in the system move from one operating point to another. The transition following a system perturbation is oscillatory in nature, but if the system is stable, the oscillations will be damped out and the system settles down at a new steady state.

The ability of all the machines in the system to adjust to small load changes is called dynamic stability of the system. If damping is insufficient, the oscillations may grow and the growing oscillations on a heavily loaded transmission line impose limitations on power transfer limit, leading to the tripping of the transmission line or forcing the under utilization of the transmission line capacity. Low frequency oscillations of sustained or growing nature have been reported in the literature by the power utilities [1,2]. These oscillations typically occur in the low frequency range of about 0.2 to 2.0 Hz. These oscillations in power can be related to oscillations of rotors of synchronous machines in the system relative to one another. In the literature these low frequency oscillations are called by different names like zero mode, inertial mode, electromechanical mode or rotor mode.

1.2 Effects of Thyristor type Excitation System on Dynamic Stability

The modern practice is to use fast acting, high gain, static excitation systems for synchronous generators. They improve the transient stability limit of the power system, but have deleterious effect on dynamic stability, resulting, often, in lightly damped and even sustained oscillations. This is more pronounced during heavy loading conditions.

de Mellow and concordia in their celebrated paper [3] have provided an insight into the effects of thyristor type excitation systems and established understanding of the stabilizing requirements of such systems.

1.3 Methods of Damping Low Frequency Oscillations

Power system engineers started serious research towards finding out means to damp out low frequency oscillations after the research work reported by de Mellow and Concordia [3]. As already mentioned, thyristor type excitation system introduces negative damping in the system. To offset this effect and to improve system damping in general, artificial means of producing torque in phase with speed are introduced using supplementary signals in the excitation control system of generators.

Additional networks are used in the excitation system to generate stabilizing signals. They are called 'Power System Stabilizers' (P.S.S.). P.S.S. introduce stabilizing signals in the excitation system. There is always a strong coupling between the voltage magnitude and reactive power in a power system. Hence P.S.S. essentially modulate reactive power to improve dynamic stability of the system.

Another method of damping the low frequency power oscillations by modulating reactive power is gaining momentum in recent years. Recent advances in thyristor technology have resulted in the emergence of a new class of devices known as 'Static VAR Compensators' (S.V.C.). The main application of such devices is to improve system voltage profile on the system by providing reactive power compensation.

Though the main function of S.V.C. is to control voltage, it has been found that a significant contribution to system damping is achieved when auxiliary feedback is introduced in the control scheme. The stabilizing signal essentially modulates the

reactive power in the system.

1.4 Objectives and Scope of This Thesis

This thesis is mainly concerned with the coordinated application of P.S.S. and S.V.C. for the improvement of dynamic stability of the power system. The main objectives of this thesis may be summarised as follows:

1. To develop a suitable model of the power system in its simplest form consisting of a generator connected to an infinite bus through a transmission line and the S.V.C. located at the mid point of the transmission line.
2. To design a P.S.S. which gives satisfactory performance over a wide range of operation, assuming that only S.V.C. voltage controller is in the system and the S.V.C. stabilizer is not present.
3. To design a S.V.C. stabilizer which gives satisfactory system performance over a wide range of operation, assuming that P.S.S. is not present in the system.
4. To study the system performance when both the S.V.C. stabilizer and P.S.S. designed independently are operated simultaneously, and to study the robustness of the system.

Robustness is one of the main requirement of the stabilizer. A stabilizer designed at an operating point should operate satisfactorily over a wide range ^{of} operating points.

1.5 Review of Literature

Extensive research has been reported in the literature concerning the application of P.S.S. for the improvement of

dynamic stability [1, 2, 3, 4, 5]. A major problem with P.S.S. design is that P.S.S. designed at one operating point may not give satisfactory performance at other operating points. To overcome this problem adaptive control techniques have been proposed by many researchers. Irving [6] describe a Modal Reference Adaptive Control (MRAC) scheme. Ghosh et al. [7] develop^d self tuning regulator for adaptive stabilization. A simple adaptive P.S.S. using gain scheduling approach has been developed by Brown Boveri [8].

Bandyopadhyay and Prabhu [9] have given a novel gain scheduling approach to adaptive P.S.S. Madhu and Prabhu [10] have adopted robustness consideration in P.S.S. design.

Application of S.V.C. for the improvement of dynamic stability is a recent development. Kinoshita [11] has reported the improvement of dynamic stability by auxiliary modulation of S.V.C. reactive power. Padiyar et al [12] have demonstrated that significant improvement in dynamic stability can be achieved by auxiliary stabilizing signal. Varma [13] has made a detailed study on the effects of S.V.C. stabilization on dynamic stability of a power system with a long transmission line. Ramar et al [14] have shown how dynamic stability can be improved using a stabilizer in S.V.C. control circuit.

Though many works have reported the application of P.S.S. alone or S.V.C. alone to improve system dynamic stability, very few research reports are available on the coordinated application of P.S.S. and S.V.C. Hamouda et al [15] have discussed the technical advantage of coordinating S.V.C. and P.S.S. for damping inertial and torsional modes of steam turbine generators,

locating S.V.C. at generator bus. C.H. Cheng et al [16] have discussed the application of P.S.S. and S.V.C. for a multimachine power system.

1.6 Location of S.V.C.

Location of S.V.C. in the power system for improvement of dynamic stability is an important problem to be carefully studied.

Hamouda et al [15] have discussed the dynamic stability enhancement by locating the S.V.C. at generator bus. Kinoshita [11], Ramar [14] and Varma [13] have discussed the dynamic stability problem by locating S.V.C. at the mid point of the transmission line, as it will boost the midpoint voltage which in turn increases the power transfer capability of the transmission line as discussed in [13].

Considering all these aspects, we have, in this thesis, located the S.V.C. at the midpoint of the transmission line.

1.7 Identifying Appropriate Signals

In the design of P.S.S. or S.V.C. stabilizer proper selection of input signal for stabilization is important.

In case of P.S.S., feedback of rotor speed deviation appears to be proper since the objective of P.S.S. is to provide adequate damping for electromechanical oscillations. Other signals such as terminal voltage, armature current, active and reactive power, field current, accelerating power, frequency etc. can also be used as P.S.S. input signals. Larsen and Swan [5] have analysed the effectiveness of speed, power and frequency signals for

P.S.S. Anwar [17] has examined the effectiveness of various P.S.S. input signals. Kundur [18] has reported the practical experience of Ontario Hydro, Canada, in P.S.S. use and has commented on the effectiveness of various P.S.S. input signals.

Several research reports have come out examining the effectiveness of various input signals for S.V.C. stabilizers. Kinoshita [11] has analysed stabilization using active power auxiliary signal for S.V.C. Padiyar et al [12] have demonstrated the efficacy of bus frequency signal for auxiliary controller. Varma [13] has compared the effectiveness of various signals such as power, frequency, reactive power in improving the dynamic stability of system with a long transmission line. He has also introduced a new auxiliary signal concept called 'Computed Internal Frequency' (CIF) and has demonstrated its superiority over other signals.

When both P.S.S. and S.V.C. are used in the system, various combination of signals can be made. Hamouda et al [15] have used modal speed as control signal for both P.S.S. and S.V.C. stabilizer. Research work has to be done to establish the effectiveness of various combinations of signals when both P.S.S. and S.V.C. are used simultaneously.

1.8 Summary of the Work Reported in this Thesis

A chapterwise summary of the work done in this thesis is given below:

Chapter 2 deals with the development of system model in state variable format for dynamic stability study. The state and output equations corresponding to P.S.S. using power and speed

8

input signals are developed. Similarly output equations corresponding to S.V.C. stabilizer using power and frequency signals are developed. A numerical example is also presented.

Chapter 3 deals with the design technique for design of P.S.S. and S.V.C. stabilizer, and methodology for coordination of PSS and SVC. An example problem is next considered and we present for it numerical results and robustness regions with P.S.S. alone, S.V.C. alone and then with both P.S.C. and S.V.C. in the system. Results are also presented with different combinations of signals.

Chapter 4 contains conclusions and suggestions for future work.

CHAPTER 2

SYSTEM MODELLING

2.1 Introduction

In the previous chapter the importance of P.S.S. and S.V.C. in damping electromechanical oscillations in power system is described. For the purpose of dynamic stability analysis, linearized model (State Space Model) of the system is used and the dynamic behaviour of the system is studied with the help of eigenvalue analysis.

The power system in its simplest form consists of a synchronous generator connected to an infinite bus through a transmission line. In the literature, various state space models of the system having varying degrees of accuracy are available. The popular Heffron-Phillip model [19] has been used by many researchers. This model is simple, and offers a good physical understanding of the synchronous generator, but does not include damper windings. Therefore the results obtained with this model are pessimistic, since a major contribution to system damping comes from damper windings [4]. Padiyar and Ramshaw [20] have developed a generalized synchronous machine model for large power system dynamic studies. This model can take into account any number of windings in the d and q axes of the rotor.

We for our study in this thesis, have considered Heffron Phillip model, as it is adequate for the purpose of dynamic stability study involving mainly the slow electromechanical and excitor mode behaviour.

2.2 Development of System Model

The state space model of the system is developed on the similar lines as in [19].

The synchronous generator is connected to an infinite bus through a transmission line and S.V.C. is installed at the midpoint of the transmission line as shown in Fig. 2.1.

The following assumptions are made for developing the state space model of the system given in Fig. 2.1:

1. The synchronous generator has no damper winding.
2. Governor-turbine dynamics can be ignored.
3. T model of the transmission line is sufficient. The line charging susceptance is clubbed with S.V.C. susceptance.
4. The machine stator and external network are in quasi-steady state.
5. Saturation in generator is neglected.

2.2.1 Generator Model

A third order generator model is considered. In the equation given below the standard notations are used.

The dynamical equation corresponding to generator field circuit can be written as [21]

$$pE_q' = -\frac{E_q'}{T_{do}} + \frac{E_{FD}}{T_{do}} + (X_d - X_d') I_d \quad (2.1)$$

The dynamical equations corresponding to the generator swing equation can be written as

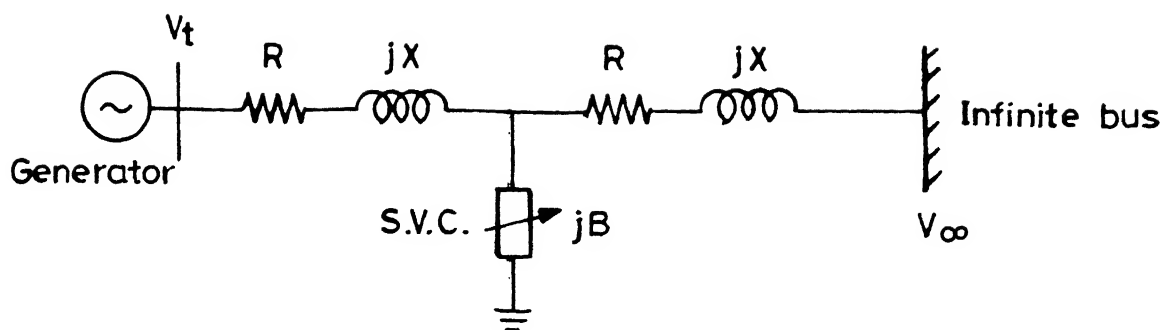


Figure 2.1 Single-machine Infinite-bus system with S.V.C.

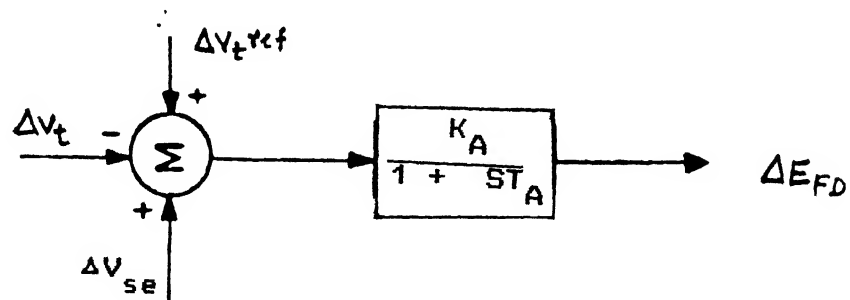


Fig. 2.2 IEEE Type-1S Excitation System

$$P\omega = \frac{1}{M} (T_m - T_e) - \frac{K_D}{M} (\omega - \omega_0) \quad (2.2)$$

$$P\delta = \omega - \omega_0 \quad (2.3)$$

where

$$M = \frac{2H}{\omega_0} \quad (2.4)$$

$$T_e = 3 (V_d I_d + V_q I_q) \quad (2.5)$$

In the equations given above δ and ω are in radians and radians/sec. The rest of the quantities are in P.U.

2.2.2 Excitation System

We are interested in the study of dynamic stability problem caused due to thyristor type excitation system. This is represented by IEEE Type 1S [22] model. Fig. 2.2 gives a block diagram representation of this excitation system.

The dynamical equation representing the excitation system is

$$PE_{FD} = - \frac{E_{FD}}{T_A} + \frac{K_A}{T_A} (V_{ref} - V_t + V_{ss}) \quad (2.6)$$

where V_t is the generator terminal voltage. It can be represented in terms of Park's voltages as

$$V_t^2 = V_d^2 + V_q^2 \quad (2.7)$$

where

$$V_d = - X_q I_q \quad (2.8)$$

$$V_q = X_q \dot{I}_d + \dot{E}_q \quad (2.9)$$

2.2.3 Static VAR Compensator (SVC)

S.V.C. is normally a combination of reactors and capacitors, controlled by thyristor circuits. Different types of S.V.C. configurations are used in practice. They are mainly:

1. Fixed capacitor and thyristor controlled reactor (FC-TCR)
2. Thyristor switched capacitor and thyristor controlled reactor (TSC-TCR).

S.V.C. configurations mentioned above are shown in Fig. 2.3. The operating principle of S.V.C. may be explained in simple terms as follows. The voltage at the bus where S.V.C. is located is continuously measured. If the voltage measured is more than the specified voltage, capacitive susceptance is presented to the system. If the voltage measured is less than the specified voltage inductive susceptance is presented to the system. This is achieved by varying the thyristor firing delay. This varies the average current flowing through the reactor and consequently makes the reactor to effectively act as a variable reactance device. The general control scheme of S.V.C. is shown in Fig. 2.4.

We have considered a simple S.V.C. voltage regulator in our modelling. Fig. 2.5 gives the block diagram representation of the S.V.C. voltage controller.

The dynamical equation representing S.V.C. voltage controller is

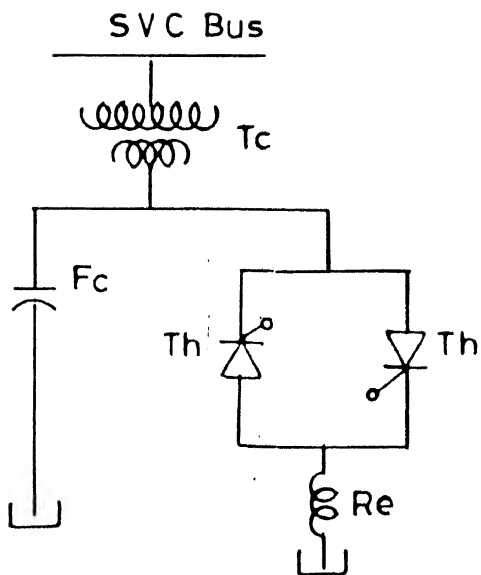


Figure 2.3(a) FC - TCR

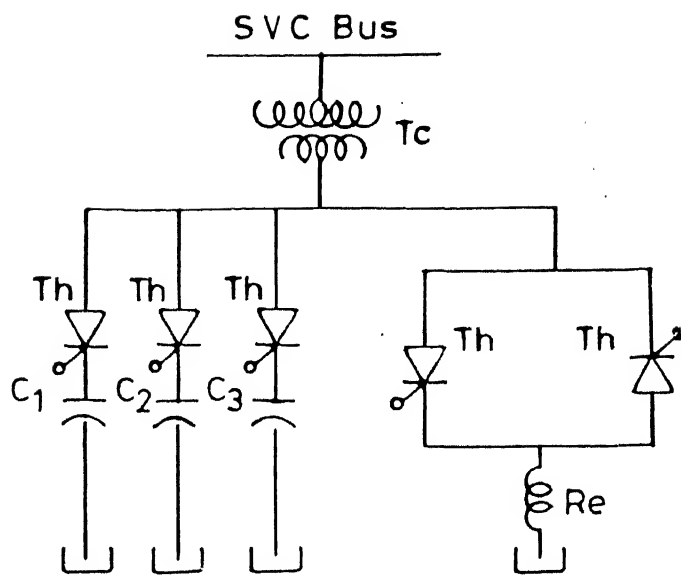


Figure 2.3(b) TSC - TCR

- F_c - Fixed capacitor
- T_c - Coupling transformer
- Th - Thyristor switch
- Re - Reactor
- C_1, C_2, C_3 Capacitors

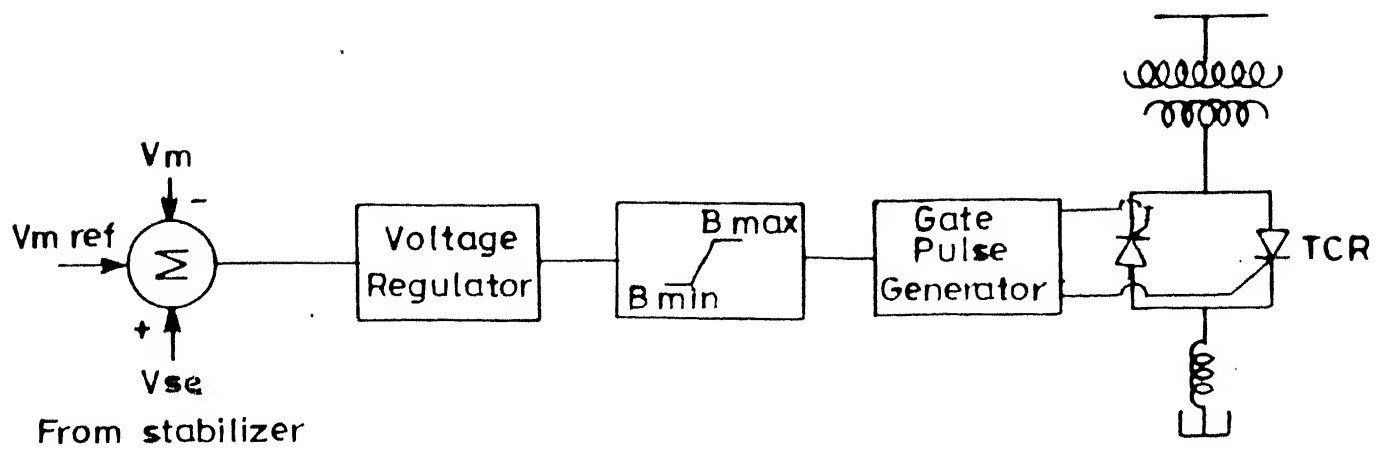


Figure 2.4 General control scheme of S.V.C.

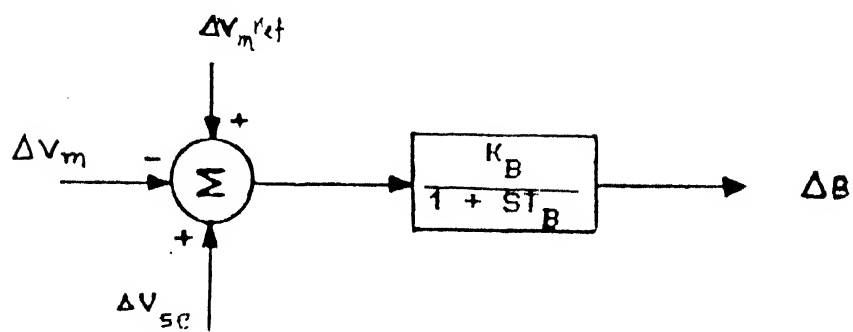


Fig. 2.5 Block Diagram Representation of SVC Voltage Controller

$$PB = - \frac{B}{T_B} + \frac{K_B}{T_B} (V_{m \text{ ref}} - V_m + V_{se}) \quad (2.10)$$

2.2.4 Linearized Model

The linearized state space model of the powersystem is obtained by linearizing eqns. (2.1), (2.2), (2.3), (2.6) and (2.10). The non-state variables ΔI_d , ΔV_t , ΔT_e and ΔV_m are then eliminated using the following expression, [derivation is given in Appendix A]

$$\begin{bmatrix} \Delta I_d \\ \Delta I_q \end{bmatrix} = \begin{bmatrix} b_{11} & b_{12} & b_{13} \\ b_{12} & b_{22} & b_{23} \end{bmatrix} \begin{bmatrix} \Delta E_q' \\ \Delta \delta \\ \Delta B \end{bmatrix} \quad (2.11)$$

where parameters b_{11}, \dots, b_{23} are defined in Appendix A.

The resulting fifth order system model is described by the state equation

$$\underline{p}\underline{x} = \underline{A}\underline{x} + \underline{b}_1 u_1 + \underline{b}_2 u_2 \quad (2.12)$$

where

$$\underline{x} = \left[\Delta E_q' \quad \Delta \omega \quad \Delta \delta \quad \Delta E_{FD} \quad \Delta B \right]^t \quad (2.13)$$

$$u_1 = \Delta V_{ss}, \text{ stabilizing signal from P.S.S.} \quad (2.14)$$

$$u_2 = \Delta V_{se}, \text{ stabilizing signal from S.V.C. stabilizer} \quad (2.15)$$

and the matrices \underline{A} , \underline{b}_1 and \underline{b}_2 are as given below:

$$A = \begin{bmatrix} A_{11} & 0 & A_{13} & A_{14} & A_{15} \\ A_{21} & A_{22} & A_{23} & 0 & A_{25} \\ 0 & A_{32} & 0 & 0 & 0 \\ A_{41} & 0 & A_{43} & A_{44} & A_{45} \\ A_{51} & 0 & A_{53} & 0 & A_{55} \end{bmatrix} \quad (2.16)$$

$$\underline{b}_1 = \begin{bmatrix} 0 & 0 & 0 & b_4 & 0 \end{bmatrix} \quad (2.17)$$

$$\underline{b}_2 = \begin{bmatrix} 0 & 0 & 0 & 0 & b_5 \end{bmatrix} \quad (2.18)$$

The parameters A_{11}, \dots, A_{55} , b_4 and b_5 in the above equation are defined in Appendix A.

2.2.5 Development of Output Equations

The output equation of the system in general can be written as

$$y_1 = c_1 \underline{x} \quad (2.19)$$

where y_1 represents the input signal to PSS, and

$$y_2 = c_2 \underline{x} + d_2 u_2 \quad (2.20)$$

where y_2 represents the input signal to the S.V.C. stabilizer. The elements of the matrices c_1 and c_2 depend upon the actual variables y_1 and y_2 chosen.

2.2.5.1 Output Equation Corresponding to PSS Input Signals

For PSS we have considered generator active power and rotor speed as control signals.

Power Signal:

Generator active power is given by

$$P_e = 3 (V_d I_d + V_q I_q) \quad (2.21)$$

In p.u., $P_e = T_e$. P_e and T_e are p.u. three phase power and torque, respectively. Hence we can write,

$$\Delta P_e = \Delta T_e \quad (2.22)$$

The output equation corresponding to power signal input PSS is then,

$$y_1 = [\Delta P_e] = \begin{bmatrix} b_{40} & 0 & b_{41} & 0 & b_{42} \end{bmatrix} \underline{x} \quad (2.23)$$

Hence,

$$c_1 = \begin{bmatrix} b_{40} & 0 & b_{41} & 0 & b_{42} \end{bmatrix} \quad (2.24)$$

where parameters b_{40} , b_{41} and b_{42} are defined in Appendix A.

Speed Signal:

Here we use change in rotor speed ($\Delta\omega$) as PSS input signal. Since speed is one of the state variables in our system model, the output equation is directly obtained as

$$\begin{aligned} y_1 &= \begin{bmatrix} \Delta\omega \end{bmatrix} \\ &= \begin{bmatrix} 0 & 1 & 0 & 0 & 0 \end{bmatrix} \underline{x} \end{aligned} \quad (2.25)$$

$$\text{Hence } c_1 = \begin{bmatrix} 0 & 1 & 0 & 0 & 0 \end{bmatrix} \quad (2.26)$$

2.2.5.2 Output Equation Corresponding to S.V.C. Stabilizer Input Signals

For S.V.C. stabilizer we have considered mid-line power and S.V.C. bus angular frequency signals.

Mid-line Power Signal:

The mid-line power is given by

$$P_m = 3 \left[V_{md} I_d + V_{mq} I_q \right] \quad (2.27)$$

Linearizing the above expression and expressing ΔI_d and ΔI_q in terms of state variables, we get

$$\Delta P_m = b_{60} \Delta E_q' + b_{61} \Delta \delta + b_{62} \Delta B \quad (2.28)$$

Thus we can write,

$$\begin{aligned} y_2 &= \begin{bmatrix} \Delta P_m \end{bmatrix} \\ &= \begin{bmatrix} b_{60} & 0 & b_{61} & 0 & b_{62} \end{bmatrix} \underline{x} \end{aligned} \quad (2.29)$$

The parameters b_{60} , b_{61} and b_{62} are defined in Appendix A.

SVC Bus Angular Frequency Signal

S.V.C. bus angular frequency ω_s is obtained as

$$\omega_s = \frac{d}{dt} \left[\tan^{-1} \frac{V_{mq}}{V_{md}} \right] \quad (2.30)$$

Linearizing the above expression,

$$\Delta\omega_s = \frac{V_{md0}}{V_{mo}^2} (p \Delta V_{mq}) - \frac{V_{mq0}}{V_{mo}^2} (p \Delta V_{md}) \quad (2.31)$$

After manipulation (see Appendix A) we can write the final expression for Δf_s as

$$\begin{aligned} y_2 &= \left[\Delta \omega_s \right] \\ &= \begin{bmatrix} b_{80} & b_{23} & b_{81} & b_{82} & b_{83} \end{bmatrix} \underline{x} + d_2 \Delta V_{se} \end{aligned} \quad (2.32)$$

Hence,

$$c_2 = \begin{bmatrix} b_{80} & b_{27} & b_{81} & b_{82} & b_{83} \end{bmatrix} \quad (2.33)$$

parameters b_{80} , b_{27} , b_{81} , b_{82} , b_{83} and d_2 are defined in Appendix A.

2.3 Numerical Example

The power system data that we have considered in this thesis are as in Ref. [11], except the excitation system data. The system is as shown in Fig. 2.6.

The generator represented in Fig. 2.6 is the equivalent generator representing all the generators of a generating station. The generator capacity is 5000 MVA. The power is transmitted over a distance of 200 km by a 500-KV two double circuit transmission lines (4 lines in parallel, in all) and SVC is installed at the mid-point of the transmission line. The power system data is given in Appendix B.

We have chosen the infinite bus as the reference bus. The S.V.C. bus voltage is specified as 1.02 p.u. Assuming that the generator is operating at rated capacity at 0.9 power factor lagging, load flow is run to compute generator terminal conditions and the S.V.C. bus voltage angle.

The A , b_1 and b_2 matrices of the system at the above operating point are

$$A = \begin{bmatrix} -0.5283 & 0 & -0.277 & 0.156 & 0.0296 \\ -106.60 & 0 & -163.76 & 0 & -2.465 \\ 0 & 1.0 & 0 & 0 & 0 \\ -1212.14 & 0 & -9.64 & -100.0 & -408.98 \\ -59.07 & 0 & 14.48 & 0 & -148.76 \end{bmatrix} \quad (2.34)$$

$$\underline{b}_1 = \begin{bmatrix} 0 & 0 & 0 & 5000 & 0 \end{bmatrix}^t \quad (2.35)$$

$$\underline{b}_2 = \begin{bmatrix} 0 & 0 & 0 & 0 & 1000 \end{bmatrix}^t \quad (2.36)$$

The open loop eigenvalues corresponding to the above A matrix are

$$-148.54, \quad -98.85, \quad -1.987, \quad -0.1116 \pm j \, 12.79$$

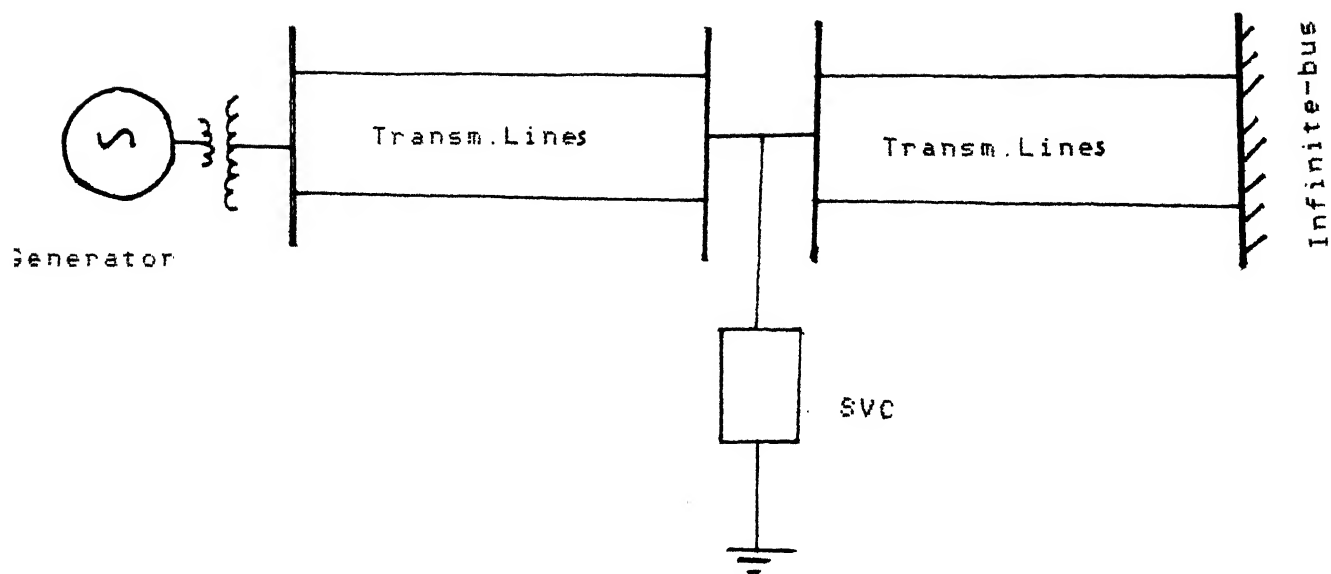


Fig. 2.6 Example System

2.4 Concluding Remarks

In this chapter, we have developed the state-space model of a single machine infinite bus system with SVC located at the midpoint of the transmission line. The output equations corresponding to various input signals of the stabilizers are developed. A numerical example is also presented.

CHAPTER 3

DESIGN OF STABILIZERS

3.1 Introduction

The state space model of the system developed in Chapter 2 is used to design the P.S.S. and S.V.C. stabilizers.

In this chapter P.S.S. and S.V.C. stabilizers are designed using the technique described in [23]. We have adopted partial pole placement technique. The choice of assigned closed loop eigenvalues, design methodology and sector criterion are discussed in this chapter. Numerical results with different signals are presented.

3.2 Problem Formulation

The main objective of either P.S.S. or S.V.C. stabilizer is to provide adequate damping for electromechanical oscillations. de Mellow and Concordia [3] have provided an insight into the dynamic stability problem of synchronous generators, in terms of synchronizing and damping torques. Synchronizing torque is the component of the electrical torque in phase with rotor angle phasor and the damping torque is the component which is in phase with rotor velocity phasor. For the system to be dynamically stable, both these torques should be positive. Thus improving dynamic stability means providing an additional damping torque component, inphase with rotor velocity. This forms the basis for the design of P.S.S. or S.V.C. stabilizer as a phase lead network as shown in Figs. 3.1 and 3.2 respectively.

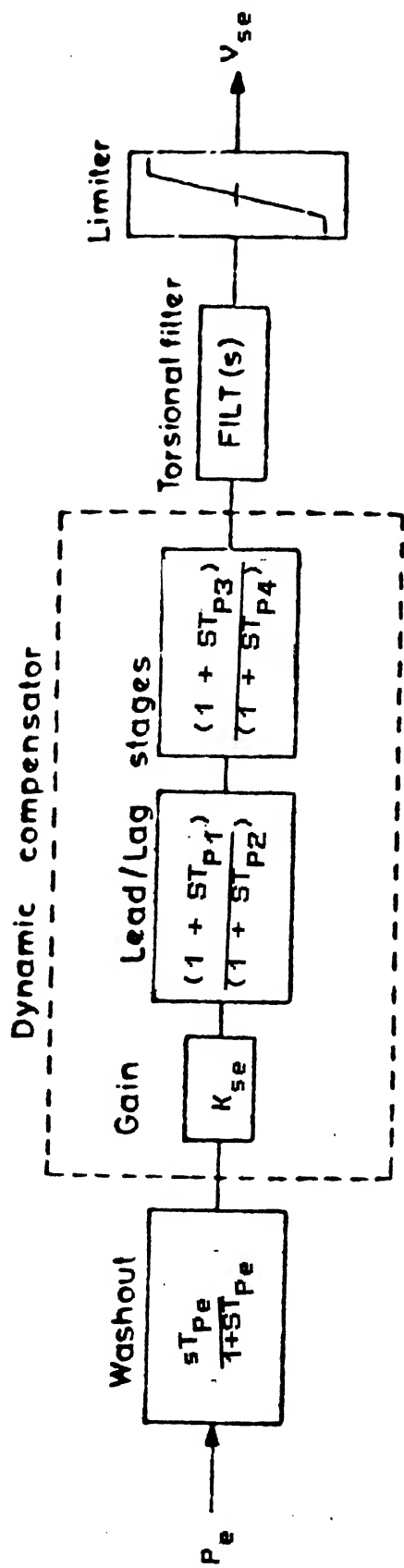


Fig. 3.1 Structure of P.S.S.

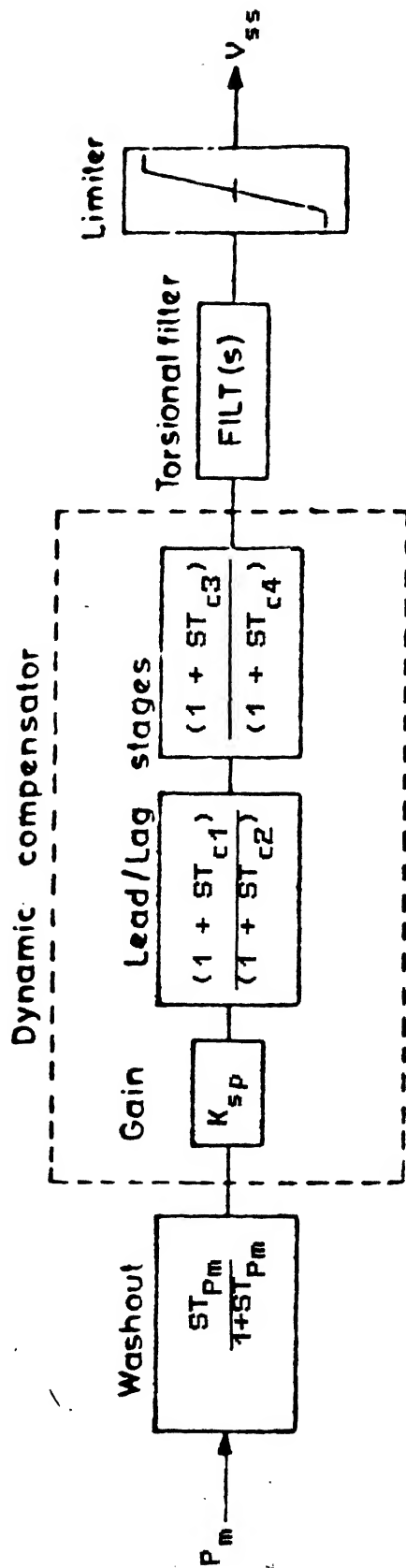


Fig. 3.2 Structure of SVC Stabilizer

Neglecting the filter and washout stages, the P.S.S. and S.V.C. stabilizers have essentially second order transfer functions as given below:

$$\text{P.S.S. : } F_p(s) = \frac{(1 + ST_{p1})(1 + ST_{p3})}{(1 + ST_{p2})(1 + ST_{p4})}$$

or

$$F_p(s) = \frac{\theta_{op}s^2 + \theta_{1p}s + \theta_{2p}}{s^2 + \gamma_{1p}s + \gamma_{2p}} \quad (3.1)$$

$$\text{S.V.C. Stabilizer: } F_c(s) = \frac{(1 + ST_{c1})(1 + ST_{c3})}{(1 + ST_{c2})(1 + ST_{c4})}$$

or

$$F_c(s) = \frac{\theta_{oc}s^2 + \theta_{1c}s + \theta_{2c}}{s^2 + \gamma_{1c}s + \gamma_{2c}} \quad (3.2)$$

3.3 Design Technique

We make use of the output feedback pole placement algorithm of Munro and Hirbod [23], presented in Appendix C for P.S.S. and S.V.C. stabilizer design. The P.S.S. or S.V.C. stabilizer design uses linearized model of the power system since improvement of system response to small disturbances is of main interest. From the control engineering point of view, the role of P.S.S. or S.V.C. stabilizer can be viewed as shifting real part of eigenvalues corresponding to electromechanical mode to more suitable locations in the complex s-plane.

Several techniques for design of stabilizers are available. But pole placement approach has the advantage that as in the classical root locus procedure, it gives the designer a feeling for system response. The algorithm of pole placement technique is simple.

The algorithm discussed in [23] provides a useful technique for the design of compensators for linear multivariable systems.

If n be the order of the open loop system, q be the number of poles (eigenvalues) to be placed, m be the number of inputs and p be the number of outputs, the problem is to find an output feedback law of the form

$$U(s) = - F(s) Y(s) \quad (3.3)$$

where $F(s)$ is a proper, rational, polynomial matrix of order r , such that q poles of the closed loop system get placed at prespecified locations. If $q < (n + r)$, the problem is referred to as partial pole placement problem. If $q = (n + r)$, it is full pole placement problem.

The order of the compensator r is related to q as

$$r \geq \left[\frac{q - \max \{ m, p \}}{\max \{ m, p \}} \right] \quad (3.4)$$

Here $[]$ means the next integer nearest to the quantity in brackets.

In our case $n = 5$, $r = 2$ and $\max \{ m, p \} = 1$ since we are considering PSS and SVC separately. Hence the number of closed loop poles that can be assigned as per eqn. (3.4) is 3. During the design of stabilizers, we have observed that if we properly

prespecify three closed loop poles, the remaining unassigned poles will be at satisfactory locations in the left half of s-plane.

In case of a single input P.S.S. or single input S.V.C. stabilizer, the transfer function matrix of eqn. (3.3) is a scalar function and has the form given in eqns. (3.1) and (3.2) respectively.

3.4 Sector Criterion for Determining Robustness

From the open loop eigenvalues presented in sec. 2.3 we observe that there is a pair of complex eigenvalues which correspond to the electromechanical mode of oscillation of the system. The real part of these eigenvalues is close to the imaginary axis in s-plane indicating that there is insufficient damping in the system. The main objective of the stabilizer is to shift these eigenvalues to a more stable location in the s-plane. The damping provided depends upon the closed loop locations of these eigenvalues.

The region of robustness has been defined with respect to the sector shown in Fig. 3.3. The system is said to remain robust with respect to parameter variations if its eigenvalues remain within the sector. Note that the damping ratio of the dominant eigenvalues will be better than 0.0735. This damping is adequate for a powersystem.

3.5 Design and Coordination Methodology

The methodology for the design of P.S.S. and S.V.C. stabilizer is essentially the same. At a design point three

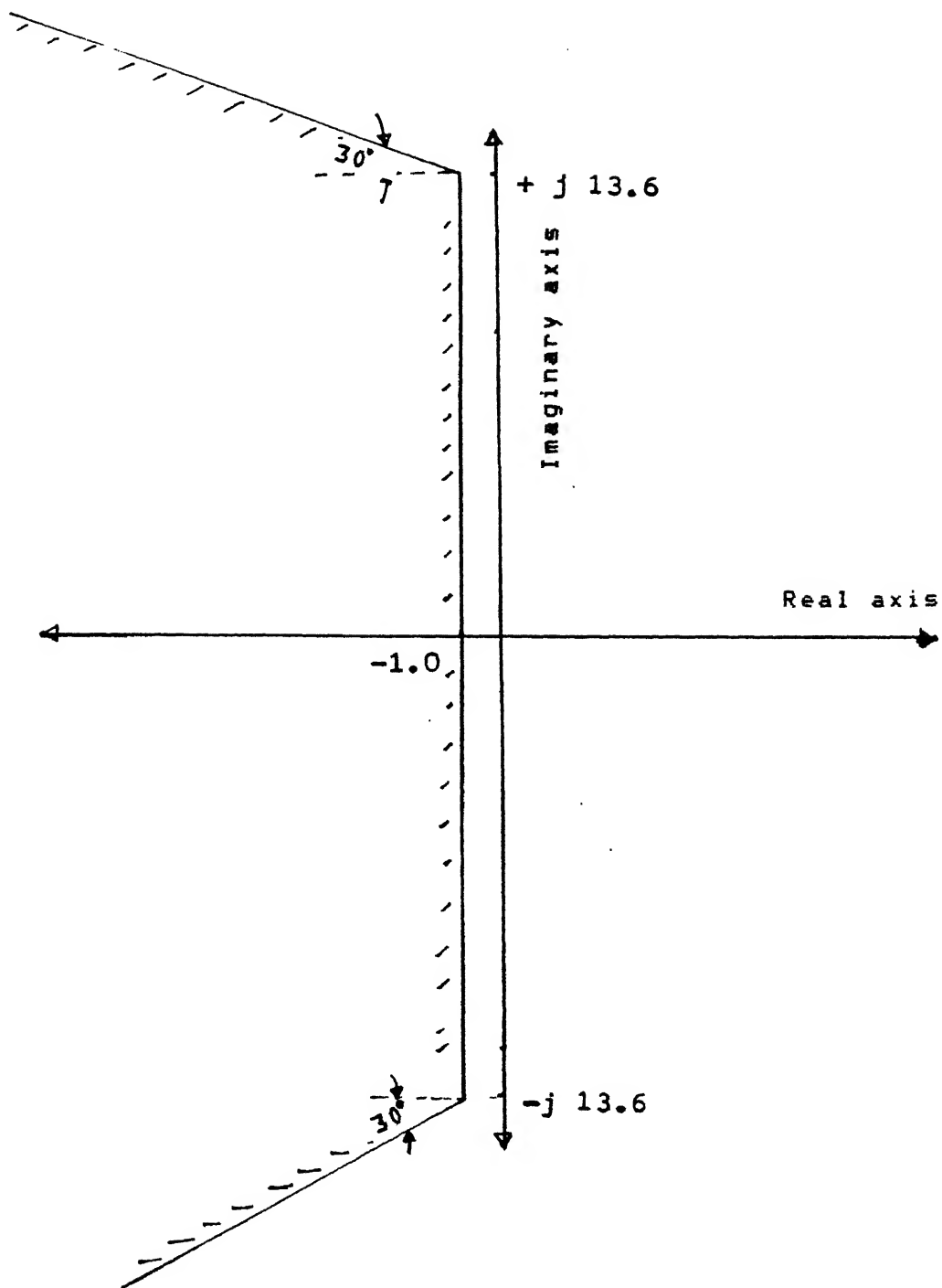


Fig. 3.3 Sector Indicating the Permissible Location of Close Loop Eigenvalues

P.S.S. and three S.V.C. stabilizers are designed independently. Then a best pair of P.S.S. and S.V.C. stabilizer is chosen for coordination from robustness point of view.

We present the design procedure adopted for P.S.S. design in detail.

3.6.1 P.S.S. Design

We have chosen a design point of 1 p.u. MVA loading at 0.9 p.f. lagging. We have chosen this design point as this is in the normal rated operating range of synchronous generator and dynamic stability under heavy loading condition is of great concern. Furthermore, the system is expected to operate near this condition most of the time. At this design point a P.S.S. is designed assuming that S.V.C. stabilizer is not in the system, using the partial pole placement algorithm given in [23]. As already mentioned under Sec. 3.3, for an open loop system of fifth order only three closed loop poles can be placed at the desired locations using a second order stabilizer. The P.S.S. denominator is prespecified such that the stabilizer poles are at stable locations. The numerator of P.S.S. transfer function is determined by prespecifying three closed loop eigenvalues to be within the sector of Fig. 3.3. Two of the eigenvalues prespecified correspond to electromechanical mode of oscillation of the system. The locations of the unassigned closed loop eigenvalues are then checked and it is ensured that they lie within the sector of Fig. 3.3

Similarly a few more P.S.S.s are designed (we have actually designed two more PSS) at the same operating point by

prespecifying three eigenvalues as in the first design explained above and choosing their locations to be different from one another but close to the corresponding location in the first design.

3.5.2 S.V.C. Stabilizer Design

After completing the P.S.S. design, several S.V.C. stabilizers (we have actually designed three stabilizers) are designed for the same design point and the same prespecified eigenvalue locations as for PSS design. The same procedure as discussed under PSS design (Sec. 3.5.1) is followed.

3.5.3 Coordination of P.S.S. and S.V.C. Stabilizer

The design of P.S.S. and S.V.C. stabilizers is complete. The region of robustness of each P.S.S. designed is determined assuming that S.V.C. stabilizer is not present. Similarly the robustness region of each S.V.C. stabilizer is determined assuming that P.S.S. is not in the system. The procedure for determining the region of robustness is as follows. The operating point of the generator is changed in all the directions of the design point in P-Q plane (where P is the generator real power and Q is the generator reactive power) keeping the stabilizer parameters unchanged. The system parameters are determined for each operating point. The region of robustness of the stabilizer is that region where all the system closed loop eigenvalues remain within the sector defined in Fig. 3.3

After completing the process of finding robustness of all stabilizers designed, it is observed that the region of

robustness of P.S.S. is normally larger than the region of robustness of S.V.C. stabilizer. Now a trial and error method is adopted to coordinate P.S.S. and S.V.C. stabilizer. First a P.S.S. is chosen, correspondingly a S.V.C. stabilizer is chosen. Both of them are switched on to the system simultaneously. The region of robustness of the pair is determined. Similarly robustness region of all the other possible pairing of P.S.S. and S.V.C. (actually eight possible pairs in our case) are determined. After completing the process, it is observed that a further improvement in the region of robustness is obtained if the P.S.S. and the S.V.C. stabilizer paired have their individual region of robustness overlapped by largest amount. On the other hand if the P.S.S. and S.V.C. stabilizer paired have their individual area of robustness quite different, the region of robustness of the pair will not be appreciable. It is normally less than the individual robustness of P.S.S.

3.6 Choice of Closed Loop Eigenvalues

The open loop system has five eigenvalues. Out of these five two are in very stable locations. The remaining three eigenvalues, two corresponding to the electromechanical mode ($0.116 \pm j12.79$) and the third corresponding to exciter mode (-1.987), are near to the imaginary axis. So we have chosen these three eigenvalues for prespecifying. The real part of the eigenvalues corresponding to electromechanical mode are shifted near to -1.5 and their imaginary parts are changed depending upon the requirement. The eigenvalue corresponding to the exciter mode is shifted near to -2.0 . The exact locations of the

prespecified eigenvalues is determined by an computer aided trial and error method keeping in mind that the unassigned poles should also lie within the sector defined in Fig. 3.3 and stabilizer gains should not be too high.

3.7 Numerical Results

For all the numerical results presented in this section, the design point is that corresponding to 0.9 p.f. lagging on 1 p.u. MVA semicircle. The open loop eigenvalues of the system corresponding to this operating point are given in section 2.3.

3.7.1 Results with P.S.S.

Here we present the numerical results obtained with PSS in the absence of SVC stabilizer. Results are presented for power input and speed input PSS.

3.7.1.1. PSS with Generator Active Power Deviation ΔP_e as Input

In this case,

$$\begin{aligned} y_1 &= \Delta P_e = c_1 x \\ &= \begin{bmatrix} b_{40} & 0 & b_{41} & 0 & b_{42} \end{bmatrix} \end{aligned} \quad (3.5)$$

where the parameters are defined in Appendix A.

Table 3.1 presents the numerical results pertaining to three PSS designed at the same design point. The result presented shows the closed loop eigenvalues assigned, transfer function and the range of robustness of each PSS on 1 p.u. MVA semicircle.

3.7.1.2 PSS with Angular Velocity Deviation $\Delta\omega$ As Input

In this case,

$$\begin{aligned} y_1 &= \Delta\omega = c_1 \underline{x} \\ &= \begin{bmatrix} 0 & 1 & 0 & 0 & 0 \end{bmatrix} \underline{x} \end{aligned} \quad (3.6)$$

Table 3.2 presents the closed loop eigenvalues assigned, transfer function and range of robustness on 1 p.u. MVA semicircle of each PSS designed.

3.7.2. Results with SVC Stabilizer

Here we present the numerical results obtained with SVC stabilizer in the absence of PSS. Results are presented for power input and frequency input SVC stabilizer.

3.7.2.1 SVC Stabilizer with Midline Active Power ΔP_m as Input

In this case,

$$\begin{aligned} y_2 &= \Delta P_m \\ &= c_2 \underline{x} \\ &= \begin{bmatrix} b_{60} & 0 & b_{61} & 0 & b_{62} \end{bmatrix} \underline{x} \end{aligned} \quad (3.7)$$

where the parameters are defined in Appendix A.

Table 3.3 presents the numerical results pertaining to three SVC stabilizers designed at the same design point as for PSS design. The result presented shows the closed loop eigenvalues assigned, the transfer function and range of robustness of each SVC stabilizer on the 1 p.u. MVA semicircle.

3.7.2.2 SVC Stabilizer with SVC Bus Frequency Deviation $\Delta\omega_s$ as Input

In this case,

$$\begin{aligned}
 y_2 &= \Delta\omega_s \\
 &= c_2 \underline{x} + d_2 u_2 \\
 &= \begin{bmatrix} b_{80} & b_{27} & b_{81} & b_{82} & b_{83} \end{bmatrix} \underline{x} + d_2 \Delta V_{se}
 \end{aligned}
 \tag{3.8}$$

where the parameters are defined in Appendix A.

Table 3.4 presents the numerical results pertaining to three SVC stabilizers designed at the same design point. The result presented shows the closed loop eigenvalues assigned, the transfer function and range of robustness of each SVC stabilizer on the 1 p.u. MVA semicircle.

3.7.3 Numerical Results with both PSS and SVC Stabilizer Coordinated

PSS designed under section 3.7.1 and SVC stabilizer designed under section 3.7.2 are coordinated according to the methodology outlined in section 3.5. Results are presented when PSS and SVS stabilizers and simultaneously operated as given below:

- (i) ΔP_e input PSS and ΔP_m input SVC stabilizer
- (ii) $\Delta\omega$ input PSS and $\Delta\omega_s$ input SVC stabilizer
- (iii) ΔP_e input PSS and $\Delta\omega_s$ input SVC stabilizer
- (iv) $\Delta\omega$ input PSS and ΔP_m input SVC stabilizer

3.7.3.1 ΔP_e Input PSS and ΔP_m Input SVC Stabilizer

Table 3.5 presents the results for the coordinated application of ΔP_e input PSS and ΔP_m input SVC stabilizer. The result presented shows the closed loop eigenvalues, transfer function of PSS and SVC stabilizer chosen for coordination and the range of robustness of 1 p.u. MVA semicircle.

Figure 3.4 shows the region of robustness for PSS alone, SVC stabilizer alone and for coordinated PSS and SVC stabilizer case.

Figure 3.5 shows the initial condition response of $\Delta\delta$ in all the three cases.

Table 3.5 presents the range of robustness on 1 p.u. MVA semicircle of all other pairing possible in this case which are not selected for coordination, and Fig. 3.6 shows the region of robustness for all such cases.

3.7.3.2 $\Delta\omega$ Input PSS and $\Delta\omega_s$ Input SVC Stabilizer

Table 3.7 presents the results for coordinated application of $\Delta\omega$ input PSS and $\Delta\omega_s$ input SVC stabilizer.

Figure 3.7 shows the region of robustness on P-Q plane.

Figure 3.8 shows the initial condition response of $\Delta\delta$.

3.7.3.3 ΔP_e Input PSS and $\Delta\omega_s$ Input SVC Stabilizer

Table 3.9 presents the results for coordinated application of ΔP_e input PSS and $\Delta\omega_s$ input SVC stabilizer.

Figure 3.10 shows the region of robustness on P-Q plane.

Figure 3.11 shows the initial condition response of $\Delta\delta$.

Table 3.10 presents the range of robustness on 1 p.u.

3 MVA semicircle of other possible pairing in this case which are not selected for coordination and Fig. 3.12 shows the region of robustness for all such cases.

3.7.3.4 $\Delta\omega$ Input PSS and ΔP_m Input SVC Stabilizer

Table 3.11 presents the results for coordinated $\Delta\omega$ input PSS and ΔP_m input SVC stabilizer.

Figure 3.13 shows the region of robustness on P-Q plane.

Figure 3.14 shows the initial condition response of $\Delta\delta$.

Table 3.12 presents the range of robustness on 1 p.u. MVA semicircle which are not selected for coordination and Fig. 3.15 shows the region of robustness for all such cases.

3.7.4 Discussion of Results

After a careful study of design and coordination results, we are able ^{to} frame the following set of rules to coordinate P.S.S. and S.V.C. stabilizer in a system.

1. Choose a design point near the rated range of the generator and design several P.S.S. and S.V.C. stabilizers independently, by pole assignment.
2. Determine the region of robustness of each P.S.S. and S.V.C. stabilizer independently.
3. Select that P.S.S. and S.V.C. stabilizer for pairing whose individual regions of robustness are large and overlap by the maximum amount. The resulting pair will further improve the system performance significantly.

Table 3.1 Numerical Results for ΔP_e Input PSS

Sl.No.	Closed loop eigenvalues assigned	PSS transfer function	Range of robustness on 1 p.u. MVA semicircle (P,Q)
1.	$-1.54 \pm j.13.2$ -2.5	$F_s(s) = \frac{0.098s^2 + 3.40s + 23.6}{s^2 + 24s + 80}$	$(0.83, 0.56)$ T_0 $(0.816, -0.57)$
2.	$-1.5 \pm j13.0$ -2.2	$F_s(s) = \frac{0.114s^2 + 3.2s + 16.6}{s^2 + 24s + 80}$	$(0.842, 0.54)$ T_0 $(0.83, -0.56)$
3.	$-1.5 \pm j12.8$ -2.0	$F_s(s) = \frac{0.08s^2 + 2.89s + 6.3}{s^2 + 24s + 80}$	$(0.76, 0.65)$ T_0 $(0.876, -0.78)$

Table 3.2 : Numerical Results for $\Delta\omega$ Input PSS

Sl.No.	Closed loop eigenvalues assigned	PSS transfer function	Range of robustness on 1 p.u. MVA semicircle (P,Q)
1.	$-2.5 \pm j13.2$ -2.0	$F_s(s) = \frac{-0.138s^2 - 0.62s - 0.51}{s^2 + 30s + 200}$	$(0.852, 0.523)$ T_0 $(0.946, -0.324)$
2.	$-2 \pm j13.0$ -2.0	$F_s(s) = \frac{-0.113s^2 - 0.426s - 0.22}{s^2 + 30s + 200}$	$(0.82, 0.572)$ T_0 $(0.96, -0.28)$
3.	$-1.5 \pm j13.6$ -2.0	$F_s(s) = \frac{-0.092s^2 - 0.81s - 1.07}{s^2 + 30s + 200}$	$(0.858, 0.513)$ T_0 $(0.902, -0.43)$

Table 3.3 : Numerical Results for ΔP_m Input SVC Stabilizer

Sl.No.	Closed loop eigenvalues assigned	S.V.C. Stabilizer transfer function	Range of robustness on 1 p.u. MVA semicircle (P,Q)
1.	$-1.5 \pm j13.0$ -2.2	$F_c(s) = \frac{-0.253s^2 - 4.4s - 10.51}{s^2 + 24s + 80}$	$(0.840, 0.542)$ T_0 $(0.952, -0.30)$
2.	$-1.54 \pm j13.4$ -2.5	$F_c(s) = \frac{-0.213s^2 - 5.136s - 15.41}{s^2 + 24s + 80}$	$(0.864, 0.50)$ T_0 $(0.946, -0.324)$
3.	$-1.5 \pm j12.8$ -2.0	$F_c(s) = \frac{-0.271s^2 - 4.086s - 7.3}{s^2 + 24s + 80}$	$(0.862, 0.506)$ T_0 $(0.92, -0.40)$

Table 3.4 : Numerical Results for $\Delta\omega$ Input SVC Stabilizer
s

Sl.No.	Closed loop eigenvalues assigned	S.V.C. Stabilizer transfer function	Range of robustness on 1 p.u. MVA semicircle (P,Q)
1.	$-1.58 \pm j10.93$ -2.2	$F_c(s) = \frac{-0.0315s^2 - 2.7s - 6.73}{s^2 + 24s + 80}$	$(0.861, 0.51)$ To $(0.944, -0.33)$
2.	$-1.5 \pm j10.89$ -2.0	$F_c(s) = \frac{-0.027s^2 - 2.67s - 5.31}{s^2 + 24s + 80}$	$(0.88, 0.475)$ To $(0.92, -0.39)$
3.	$-1.54 \pm j13.2$ -2.5	$F_c(s) = \frac{-0.046s^2 - 2.8s - 8.4}{s^2 + 24s + 80}$	$(0.834, 0.55)$ To $(0.962, 0.273)$

Table 3.5 Numerical Results for Coordinated ΔP_e Input PSS
and ΔP_m Input SVC Stabilizer

Transfer functions of PSS and SVC stabilizer chosen for coordination	Location of closed loop eigenvalues	Range of robustness on 1 p.u. MVA semicircle (P,Q)
PSS	-140.2	
$F_s(s) = \frac{0.08s^2 + 2.89s + 6.3}{s^2 + 24s + 80}$	- 78.3	(0.7, 0.71)
	- 3.14 ± j12.4	To
	- 22.59	(0.86, -0.51)
	- 2.0	
	- 5.22	
SVC stabilizer	- 20.23	
$F_c(s) = \frac{-0.271s^2 - 4.08s - 7.3}{s^2 + 24s + 80}$	- 3.99	

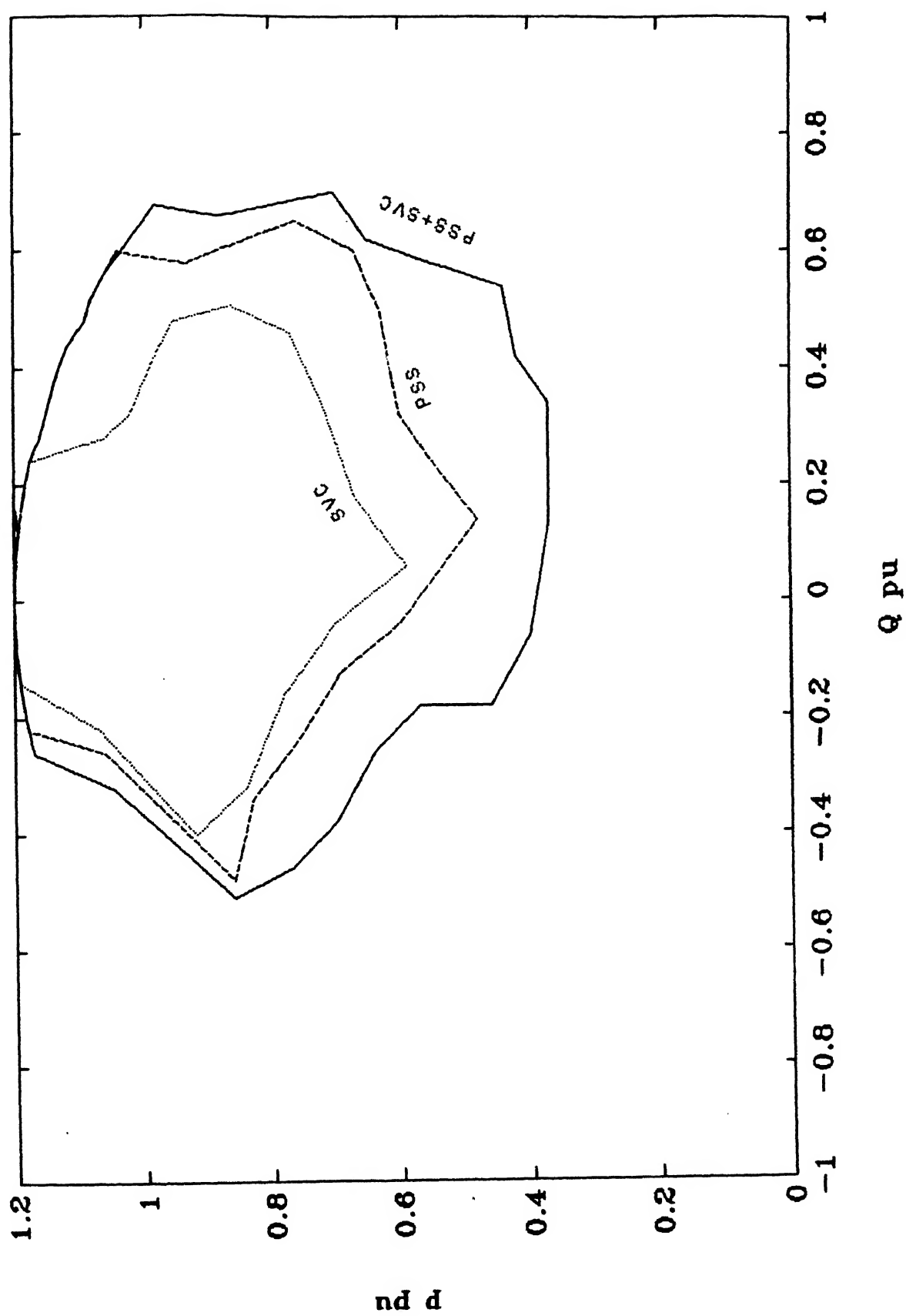


Fig. 3.4 Region of Robustness for ΔP_e Input PSS and ΔP_m Input SVC Stabilizer

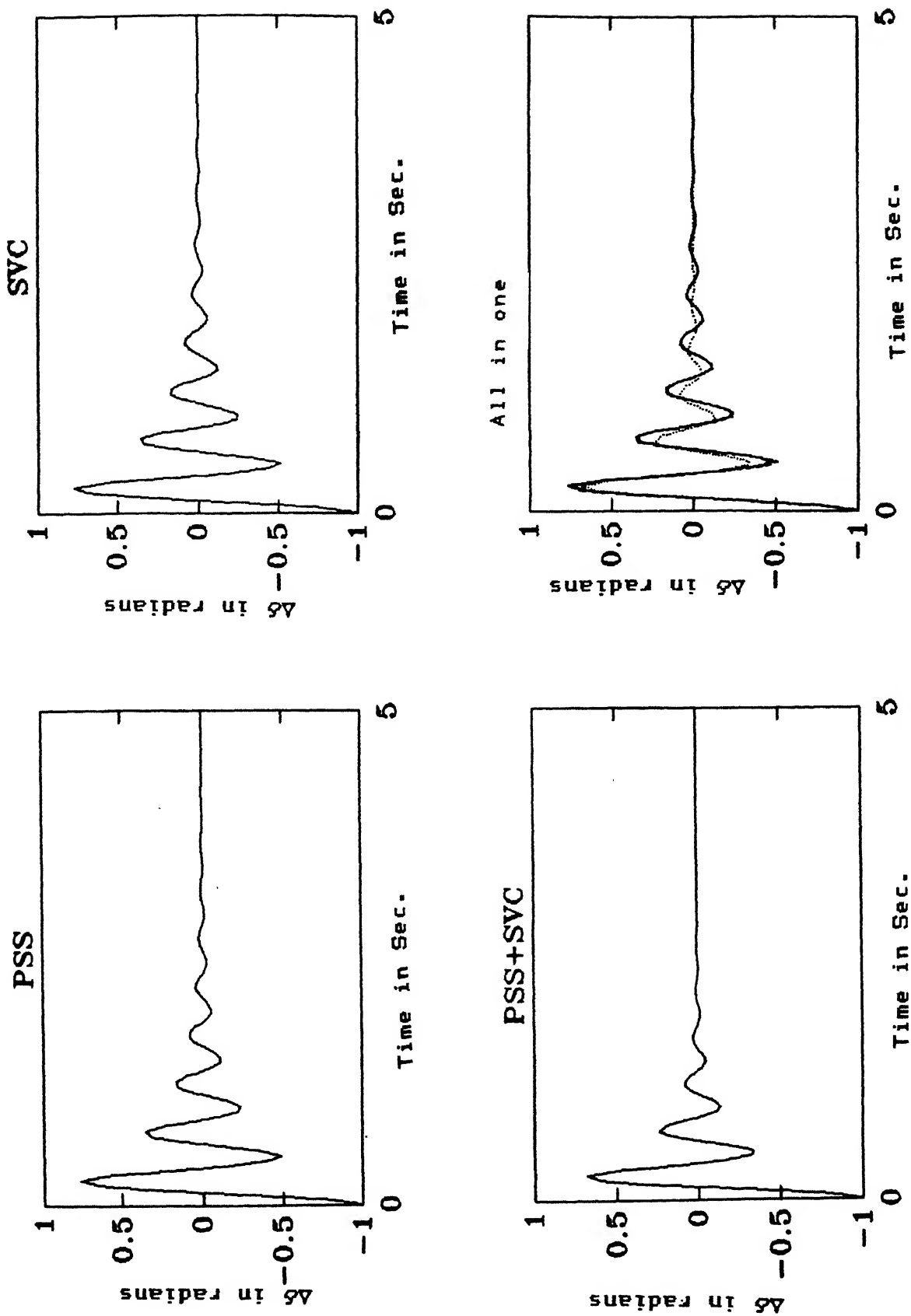


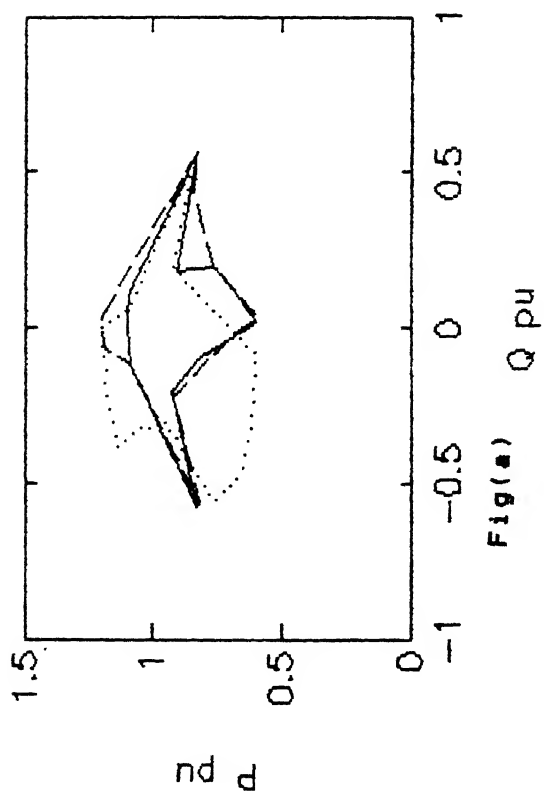
Fig. 3.5 Initial Condition Response of $\Delta\delta$; ΔP_e Input
PSS, ΔP_m Input SVC Stabilizer

Table 3.6 Numerical Results for Other Pairs of ΔP_e input P.S.S.
and ΔP_m input S.V.C. Stabilizer not
Selected for Coordination

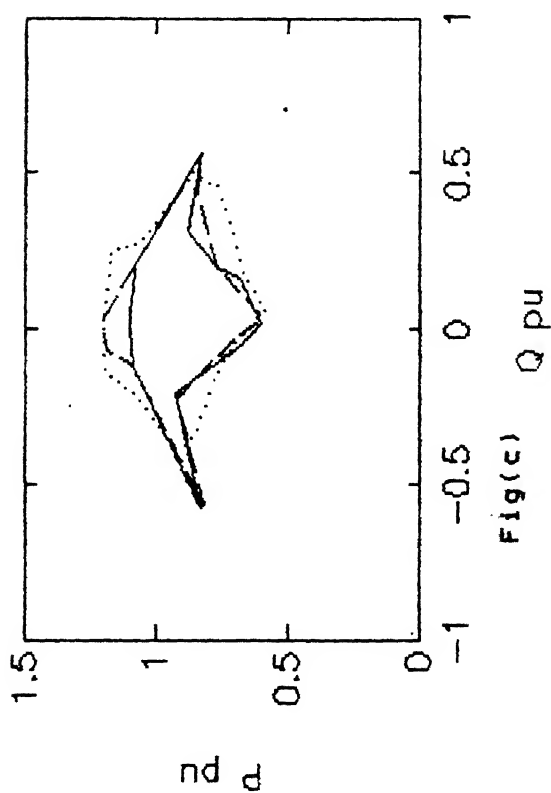
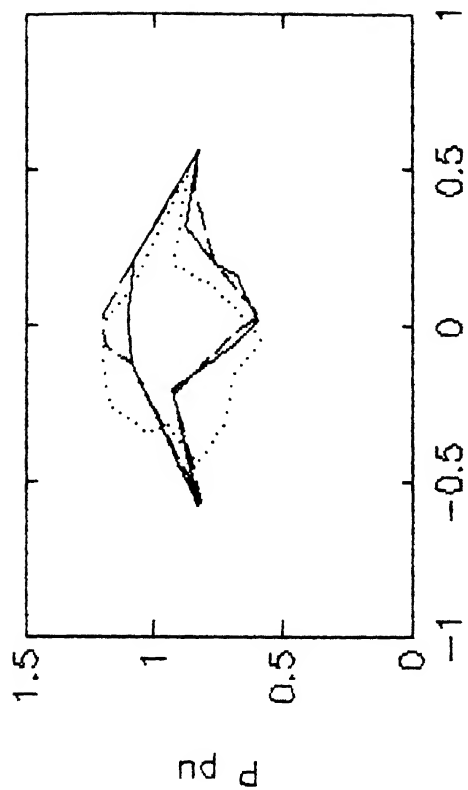
Sl.No of P.S.S. chosen from Table 3.1	Sl.No of S.V.C. Stabilizer chosen from Table 3.3	Range of robustness on 1 p.u. MVA semicircle (P , Q)	Sub-Fig.No. under Fig. No 3.6
1	1	(0.83 , 0.56) to (0.82 , -0.57)	Fig.(a)
1	2	(0.84 , 0.54) to (0.83 , -0.56)	Fig.(b)
1	3	(0.76 , 0.65) to (0.86 , -0.48)	Fig.(c)
2	1	(0.84 , 0.54) to (0.98 , -0.22)	Fig.(d)
2	2	(0.84 , 0.54) to (0.965 , -0.26)	Fig.(e)
2	3	(0.84 , 0.54) to (0.91 , -0.42)	Fig.(f)
3	1	(0.80 , 0.6) to (0.91 , -0.42)	Fig.(g)
3	2	(0.80 , 0.6) to (0.89 , -0.46)	Fig.(h)

Fig. 3.6 Region of Robustness for ΔP_m Input PSS and ΔP_m Input
SVC Stabilizer not selected for coordination

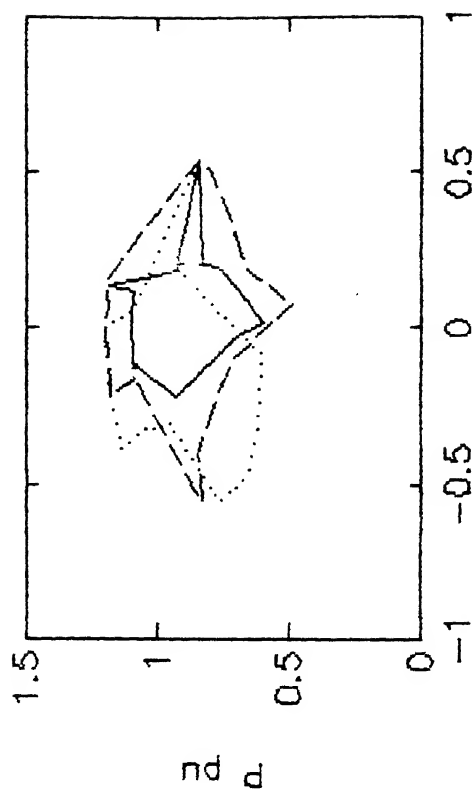
— PSS
 SVC
 — PSS+SVC



Fig(b) $Q \text{ pu}$



Fig(d) $Q \text{ pu}$



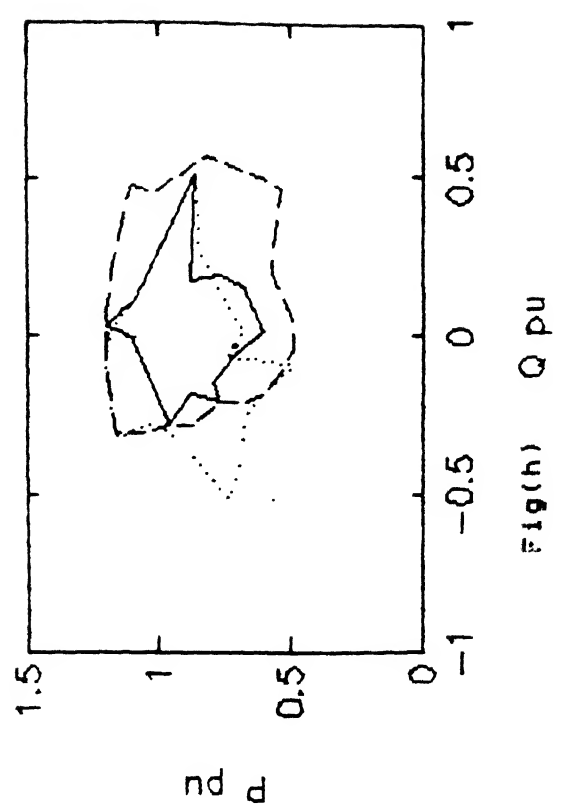
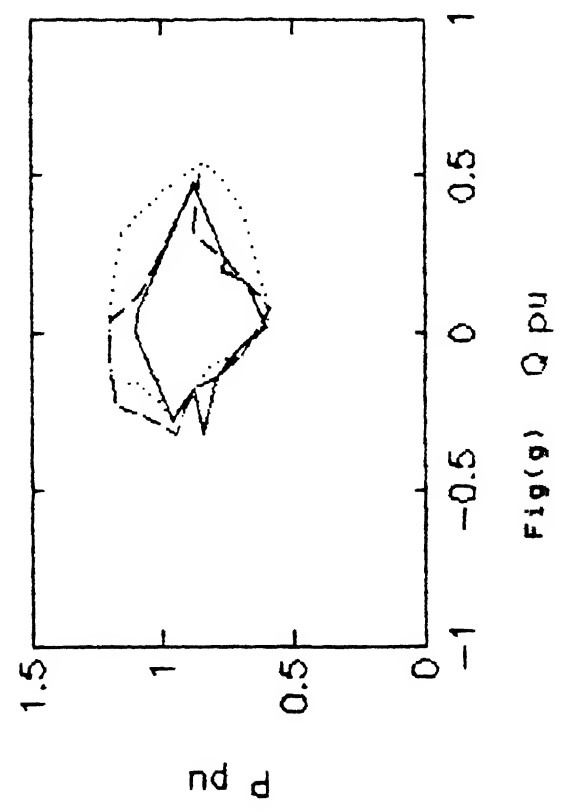
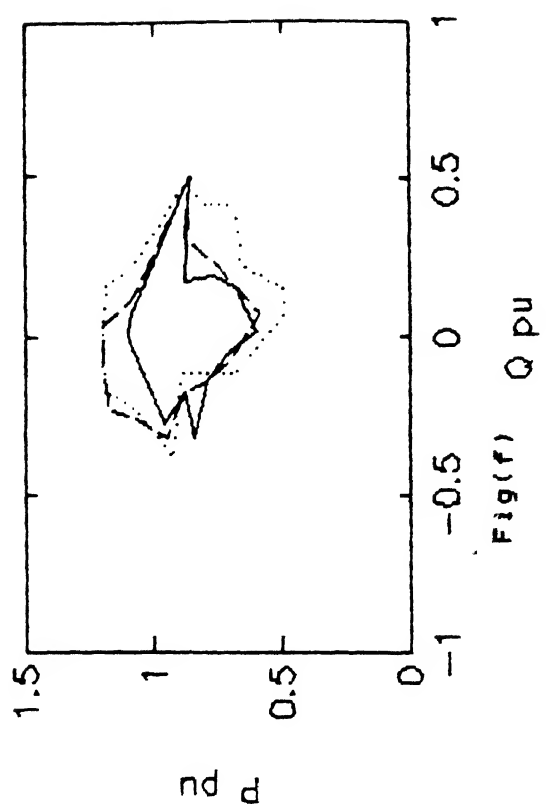
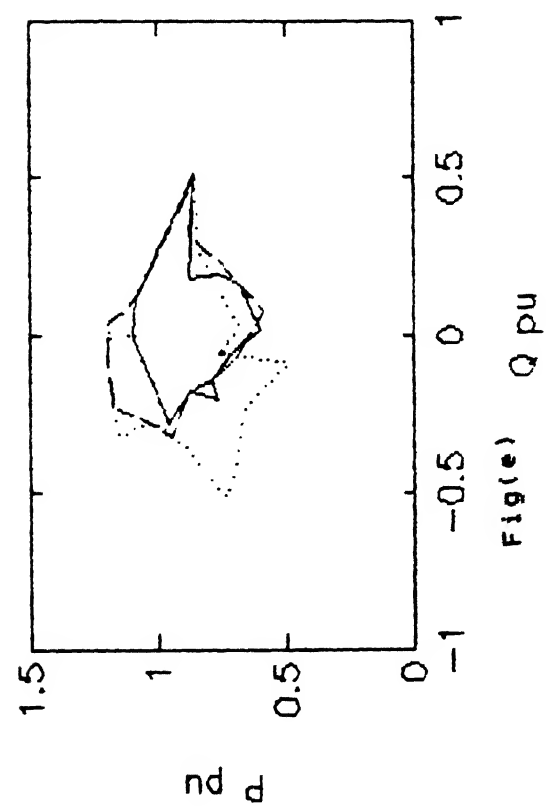


Table 3.7 Numerical Results for Coordinated $\Delta\omega$ Input PSS and $\Delta\omega_s$ Input SVC Stabilizer

Transfer functions of PSS and SVC stabilizer chosen for coordination	Location of closed loop eigenvalues	Range of robustness on 1 p.u. MVA semicircle (P,Q)
PSS	-249.5	
$F_s(s) = \frac{-0.113s^2 - 0.426s - 0.22}{s^2 + 30s + 200}$	- 95.58 - 22.69 - $3.18 \pm j11.5$ - 5.26	(0.782, 0.62) To (0.942, -0.33)
SVC stabilizer	- 4.82	
$F_c(s) = \frac{-0.046s^2 - 2.8s - 84}{s^2 + 24s + 80}$	- 2.48	

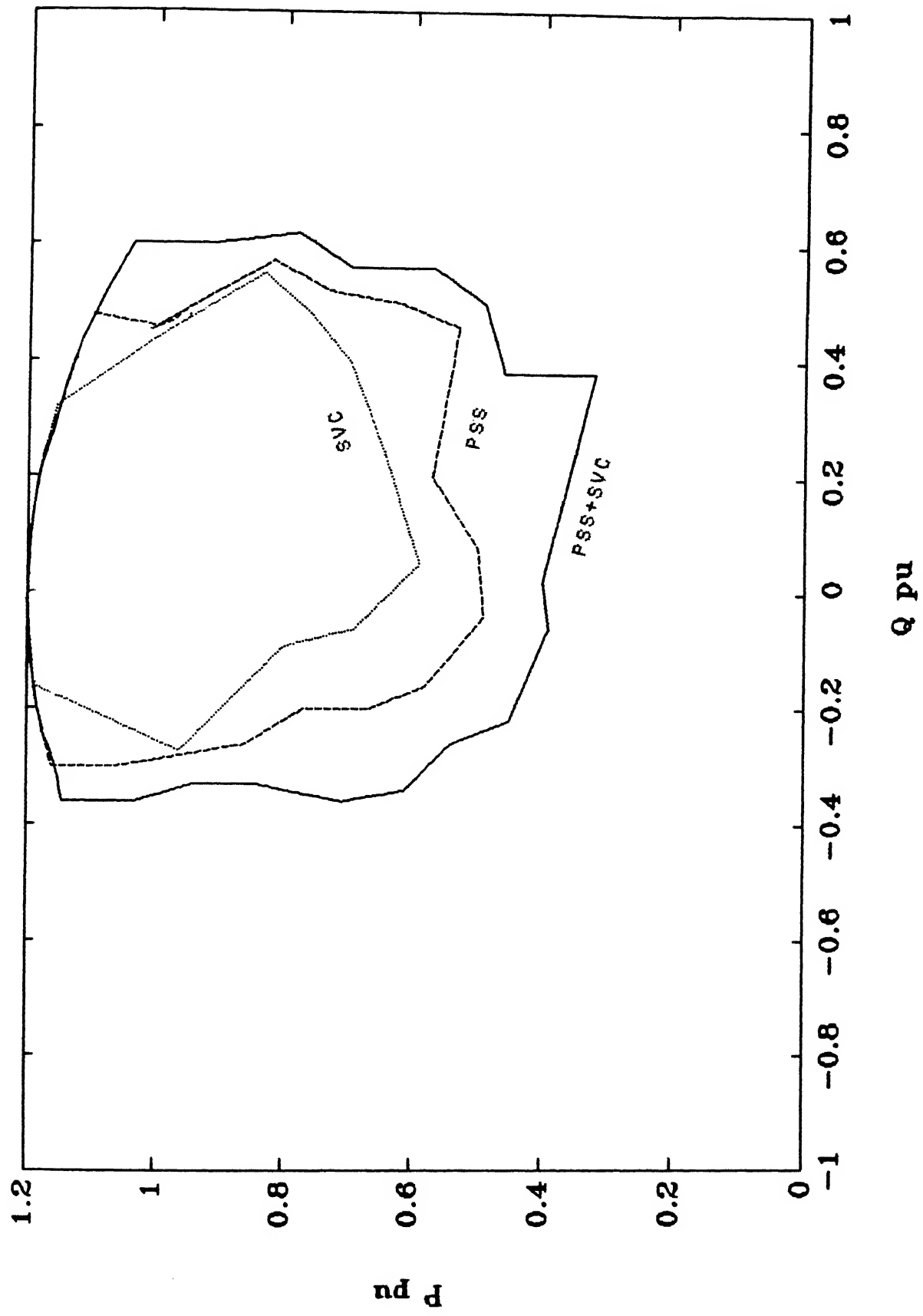


Fig. 3.7 Region of Robustness for $\Delta\omega$ Input PSS and $\Delta\omega_s$ Input SVC Stabilizer

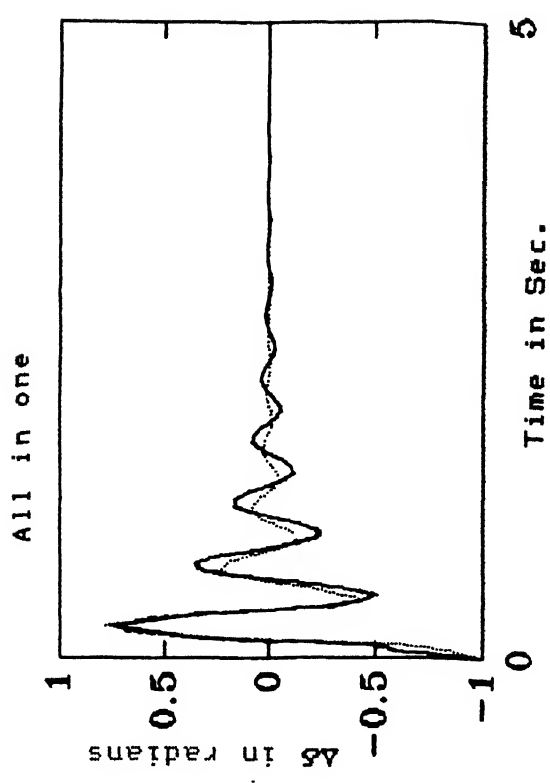
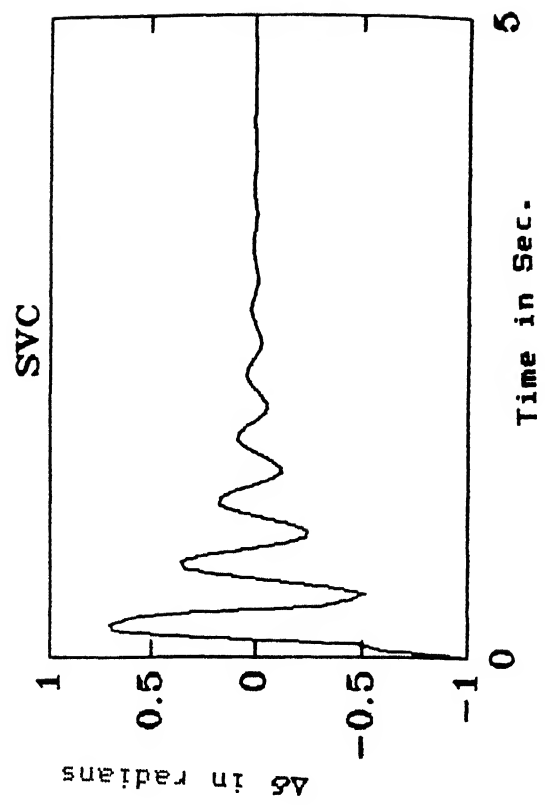
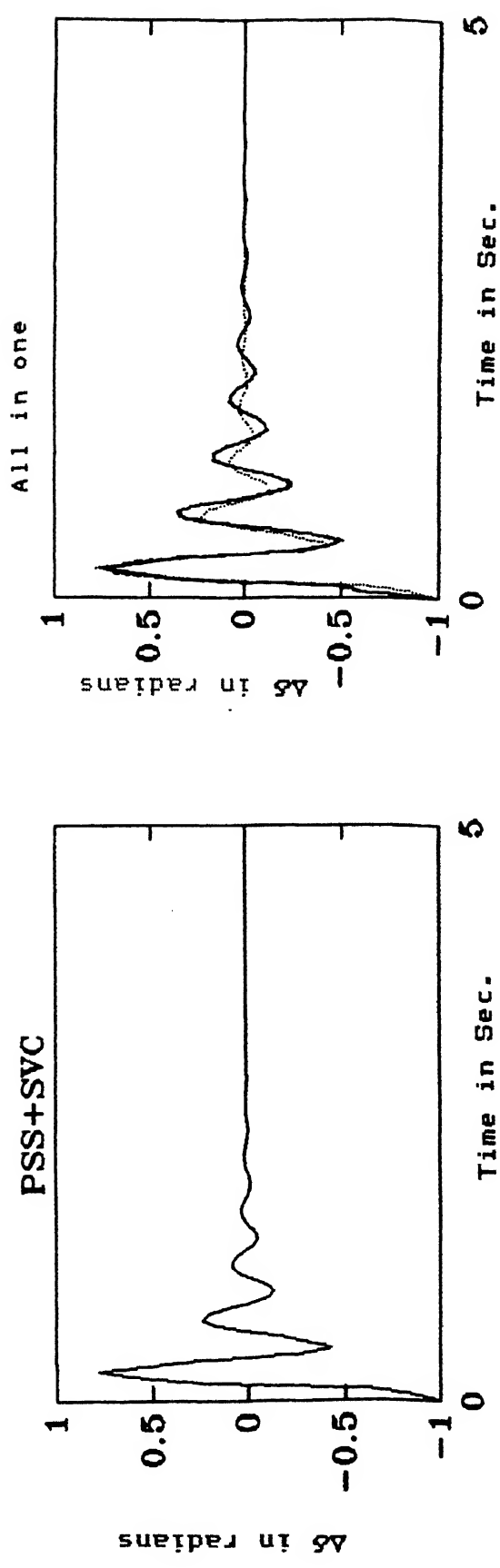
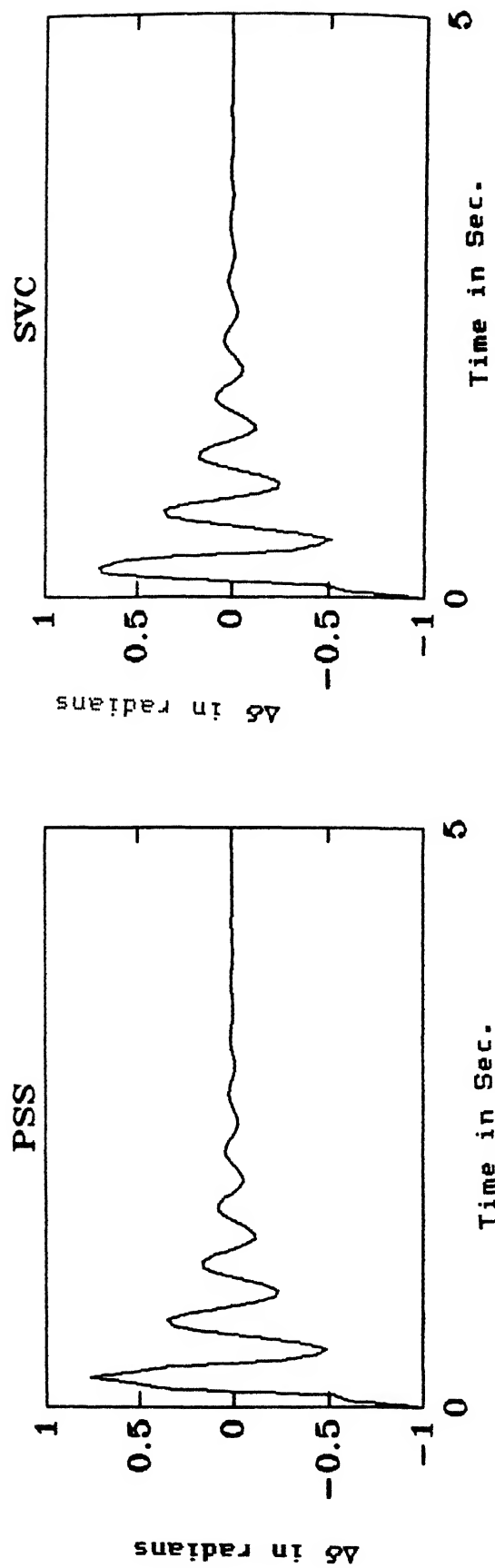
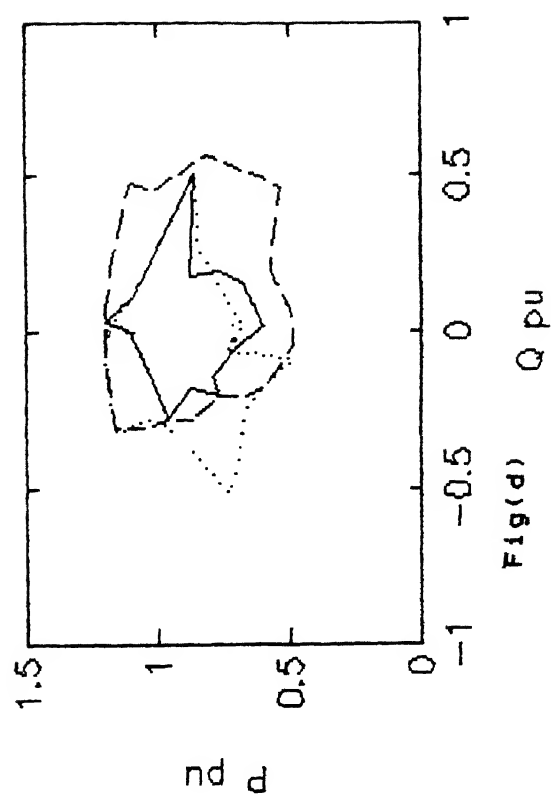
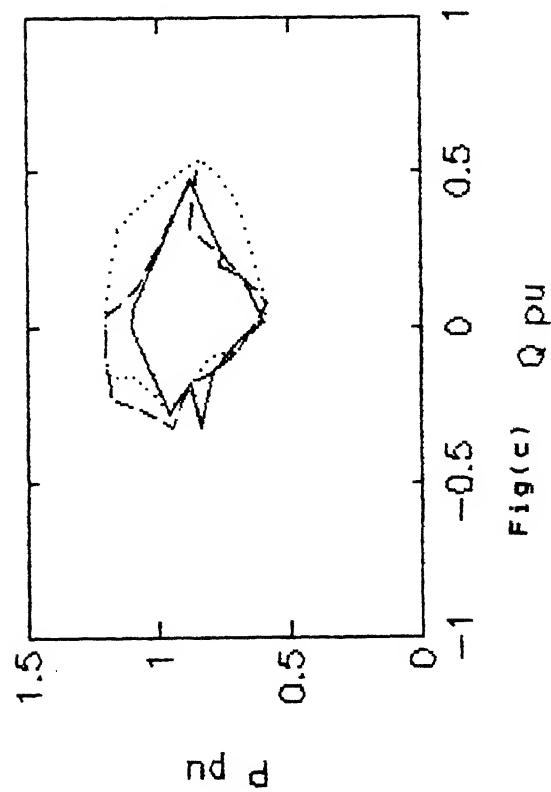
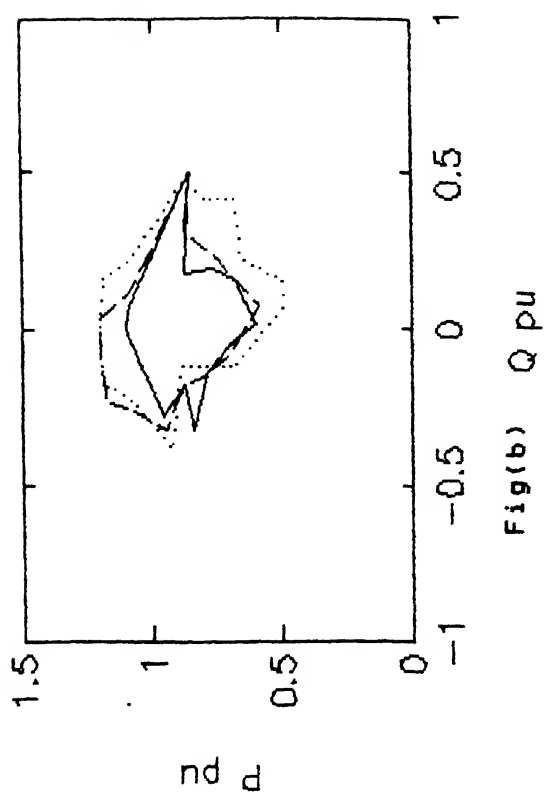
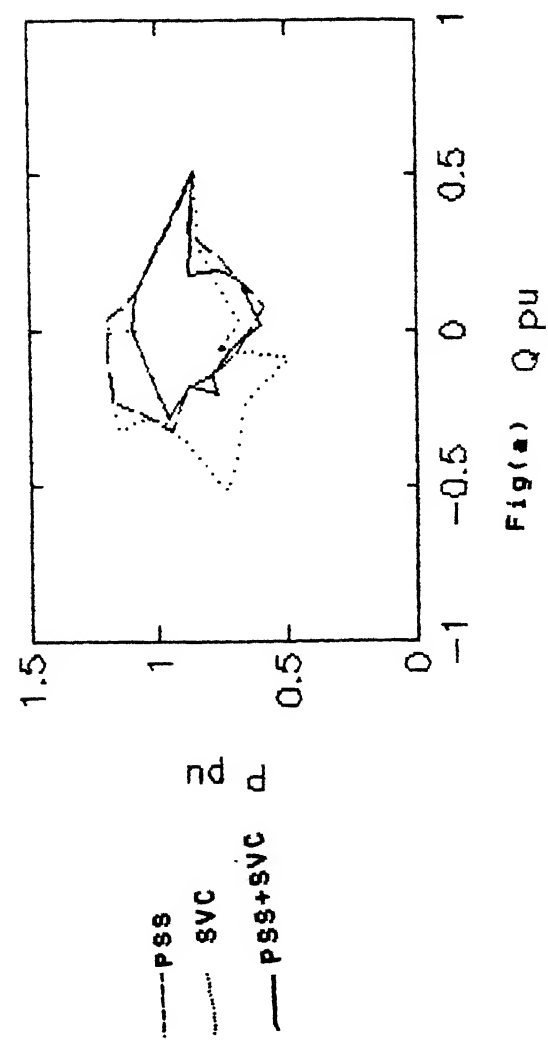


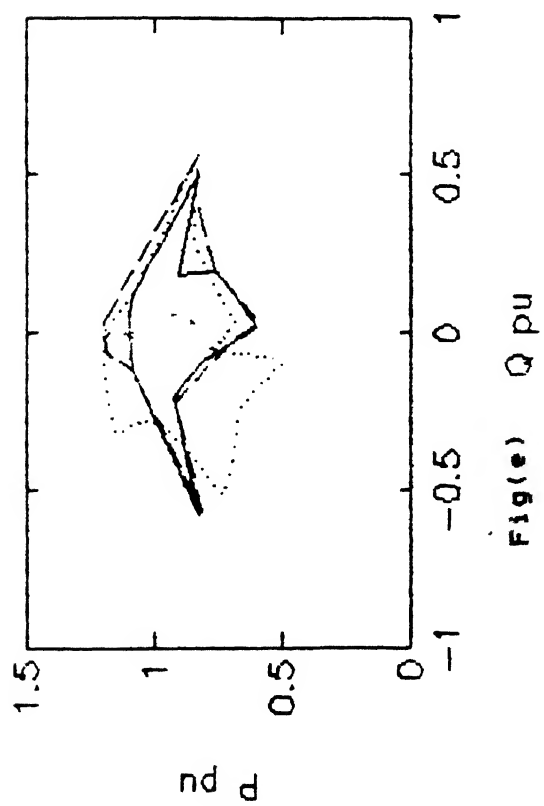
Fig. 3.8 Initial Condition Response of $\Delta\delta$; $\Delta\omega$ Input
PSS, $\Delta\omega_s$ Input SVC Stabilizer

Table 3.8 Numerical Results for Other Pairs of $\Delta\omega$ input P.S.S.
and $\Delta\omega_s$ input S.V.C. Stabilizer not
Selected for Coordination

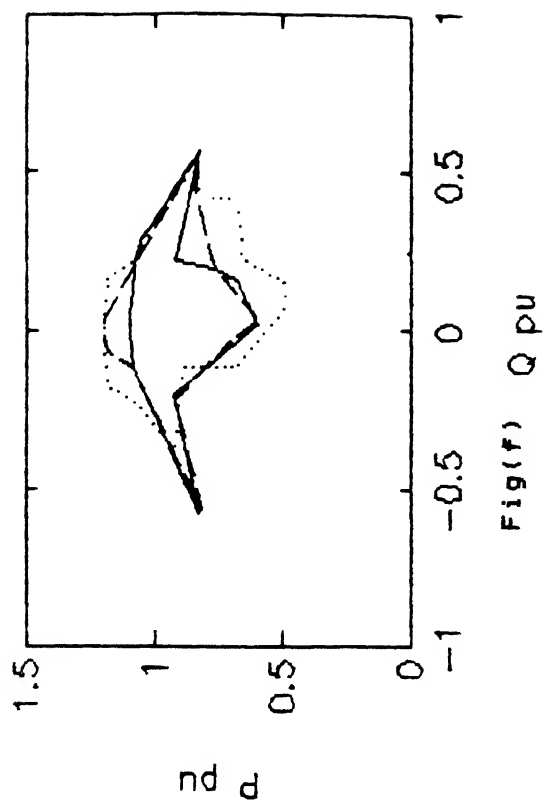
Sl.No of P.S.S. chosen from Table 3.2	Sl.No of S.V.C. Stabilizer chosen from Table 3.4	Range of robustness on 1 p.u. MVA semicircle (P , Q)	Sub-Fig.No. under Fig. No 3.9
1	1	(0.85 , 0.54) to (0.96 , -0.28)	Fig.(a)
1	2	(0.85 , 0.54) to (0.95 , -0.30)	Fig.(b)
1	3	(0.85 , 0.5) to (0.95 , -0.3)	Fig.(c)
2	1	(0.846 , 0.53) to (0.96 , -0.28)	Fig.(d)
2	2	(0.858 , 0.513) to (0.96 , -0.28)	Fig.(e)
3	1	(0.858 , 0.513) to (0.946 , -0.324)	Fig.(f)
3	2	(0.858 , 0.513) to (0.946 , -0.324)	Fig.(g)
3	3	(0.858 , 0.513) to (0.98 , -0.19)	Fig.(h)

Fig. 3.9 Region of Robustness for $\Delta\omega$ Input PSS and $\Delta\omega_s$
Input SVC Stabilizer not selected for coordination

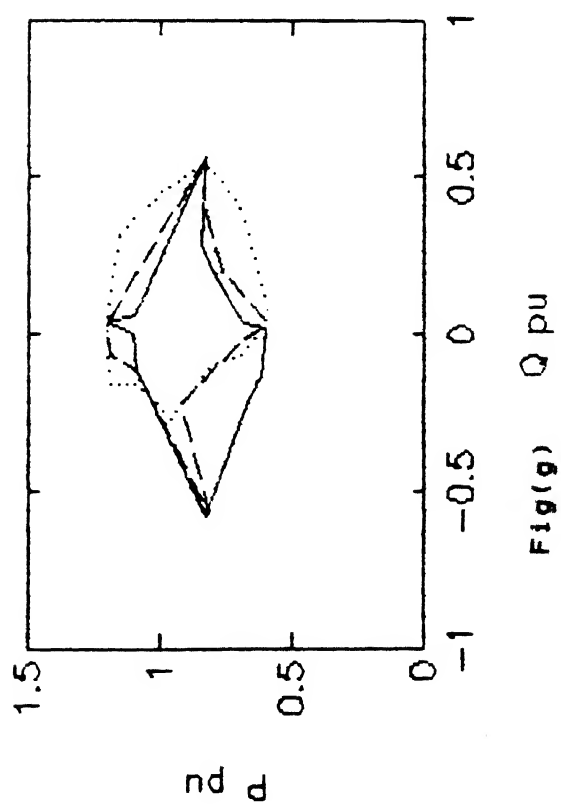




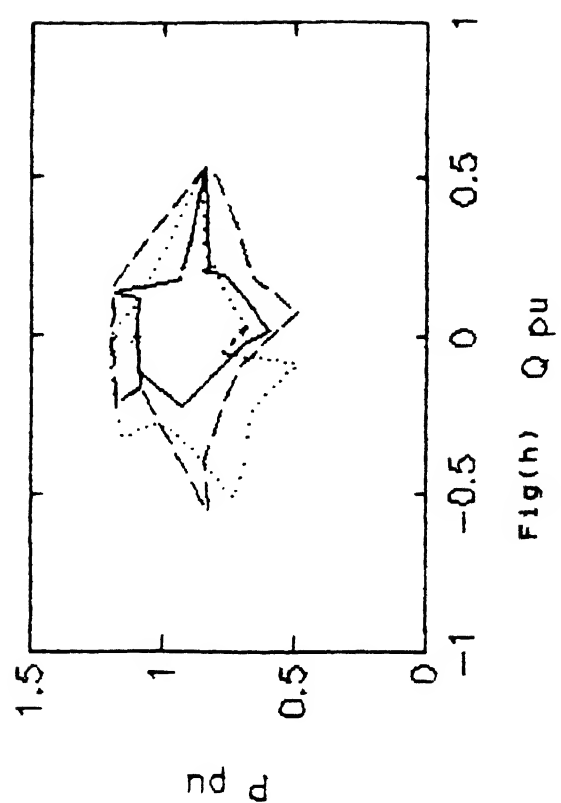
Fig(e) Q_{pu}



Fig(f) Q_{pu}



Fig(g) Q_{pu}



Fig(h) Q_{pu}

Table 3.9 Numerical Results for Coordinated ΔP_e Input PSS
and $\Delta \omega_e$ Input SVC Stabilizer

Transfer functions of PSS and SVC stabilizer chosen for coordination	Location of closed loop eigenvalues	Range of robustness on 1 p.u. MVA semicircle (P,Q)
PSS	-176.3	
$F_s(s) = \frac{0.08s^2 + 2.89s + 6.3}{s^2 + 24s + 80}$	- 97.3	(0.744, 0.67)
	- 21.8	To
	- $3.76 \pm j11.46$	(0.84, -0.54)
	- 6.46	
SVC stabilizer	- 4.2	
$F_c(s) = \frac{-0.027s^2 - 2.67s - 5.31}{s^2 + 24s + 80}$	- 2.49	
	- 3.98	

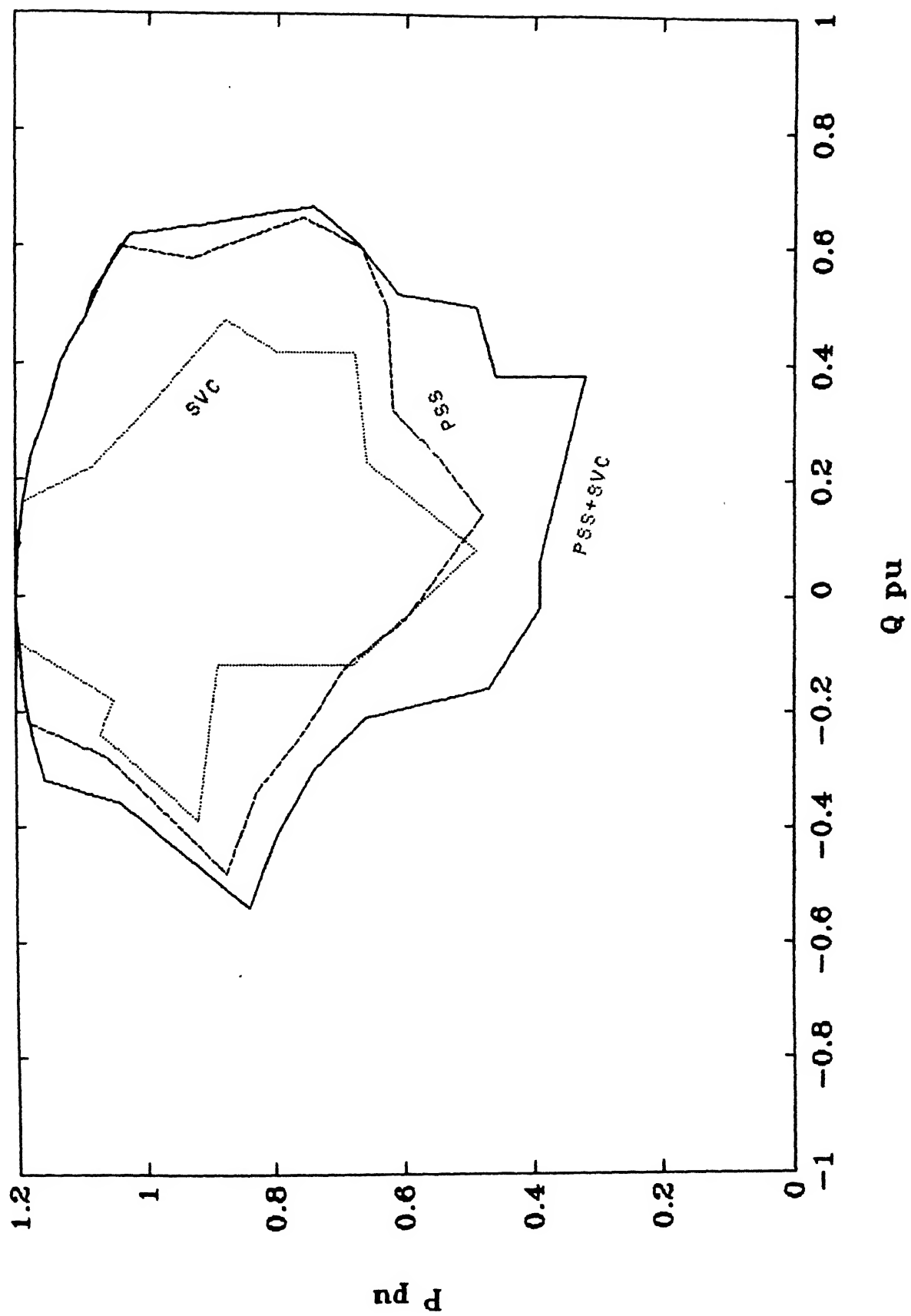


Fig. 3.10 Region of Robustness for ΔP_e Input PSS and $\Delta \omega_s$ Input SVC Stabilizer

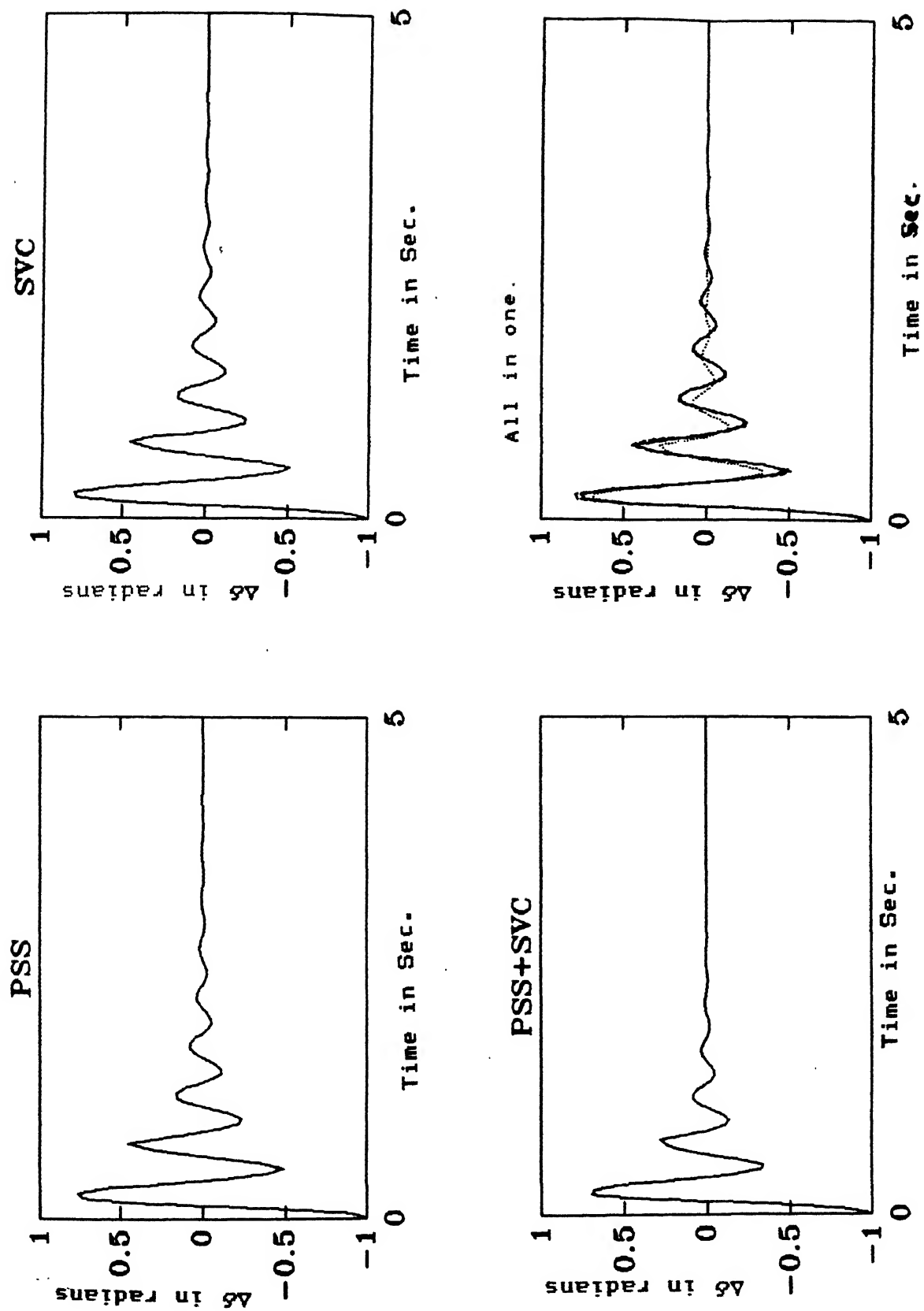
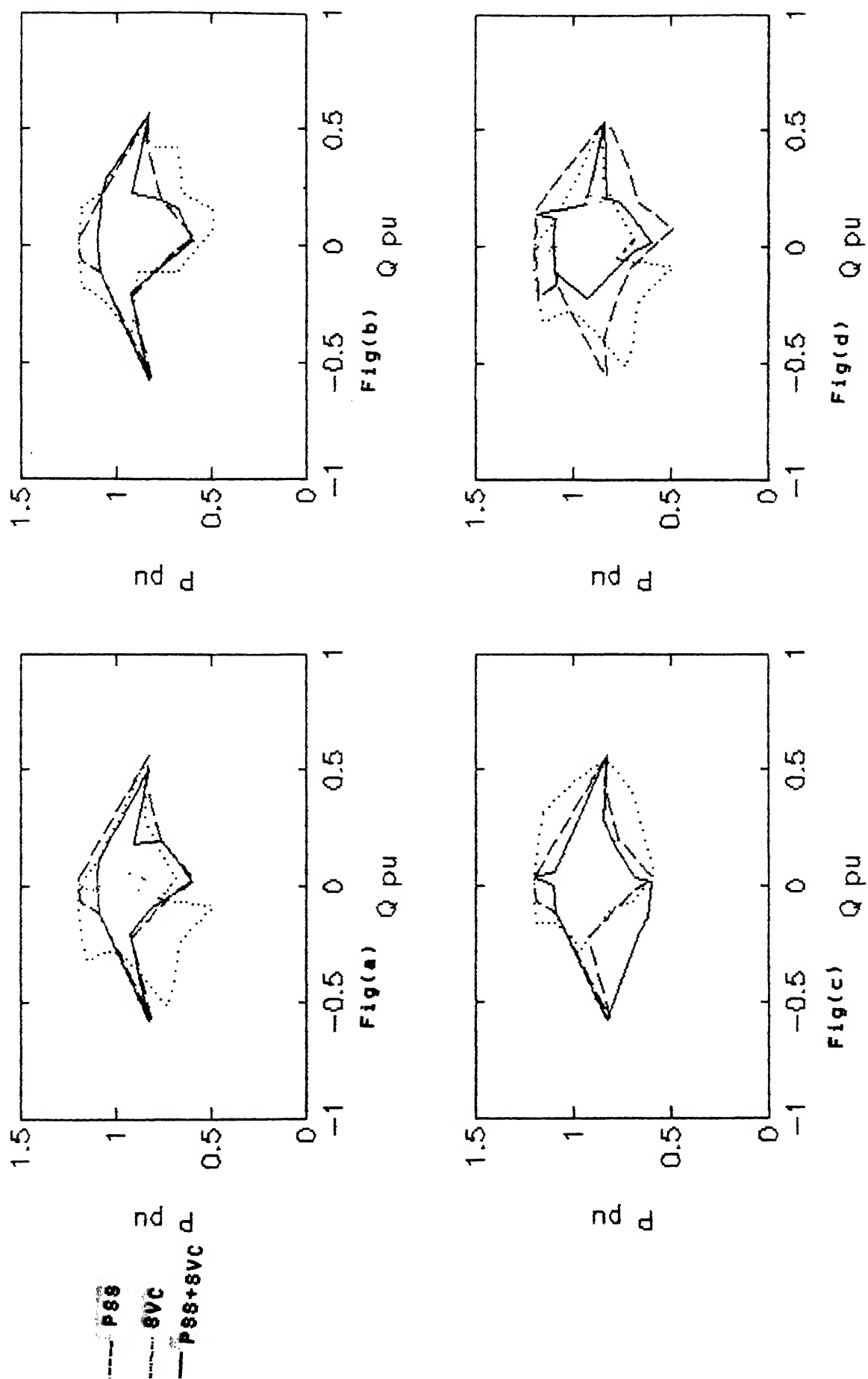
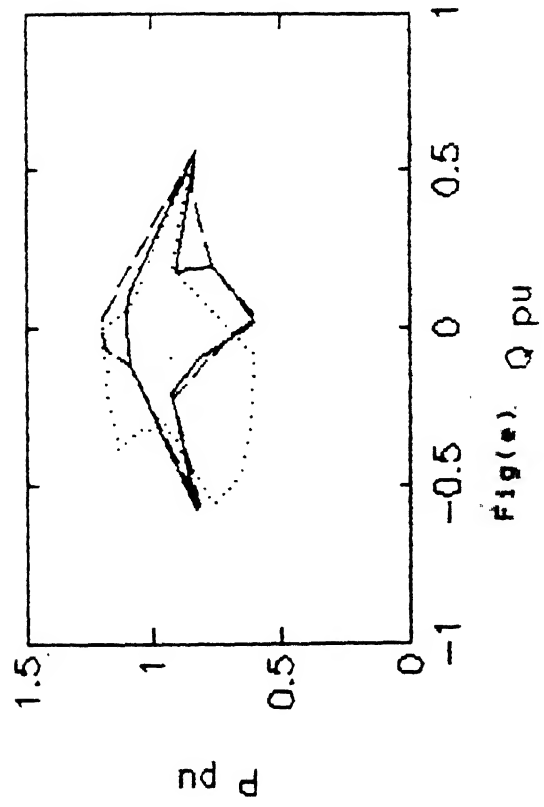


Fig. 3.11 Initial Condition Response of $\Delta\delta$; ΔP_e Input
PSS, $\Delta\omega_s$ Input SVC Stabilizer

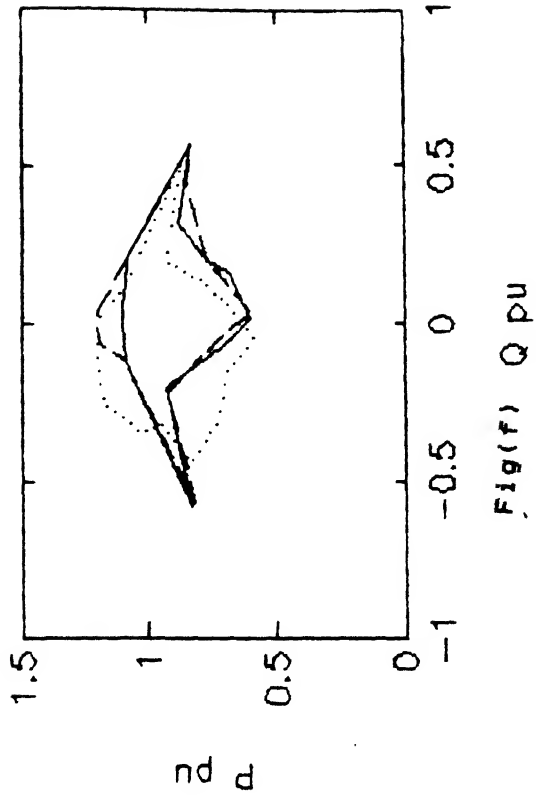
Fig. 3.12 Region of Robustness for ΔP_e Input PSS and

$\Delta\omega_3$ Input SVC Stabilizer not selected for coordination

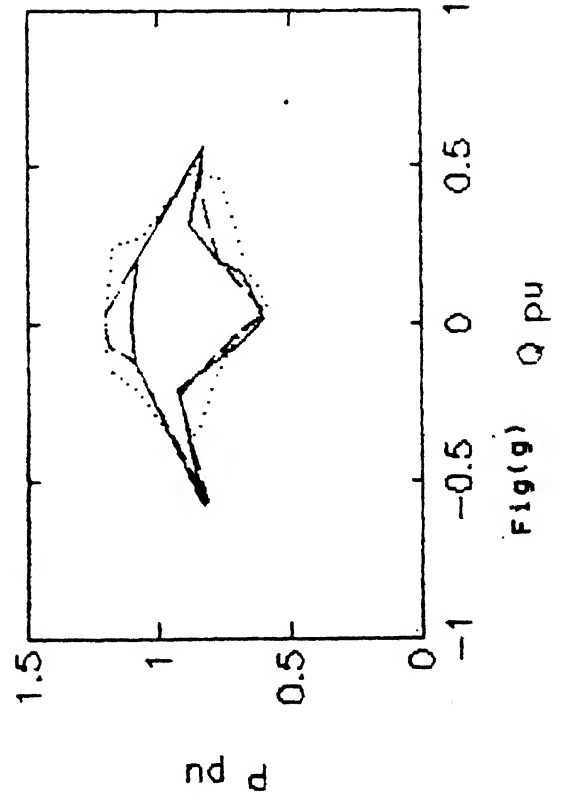




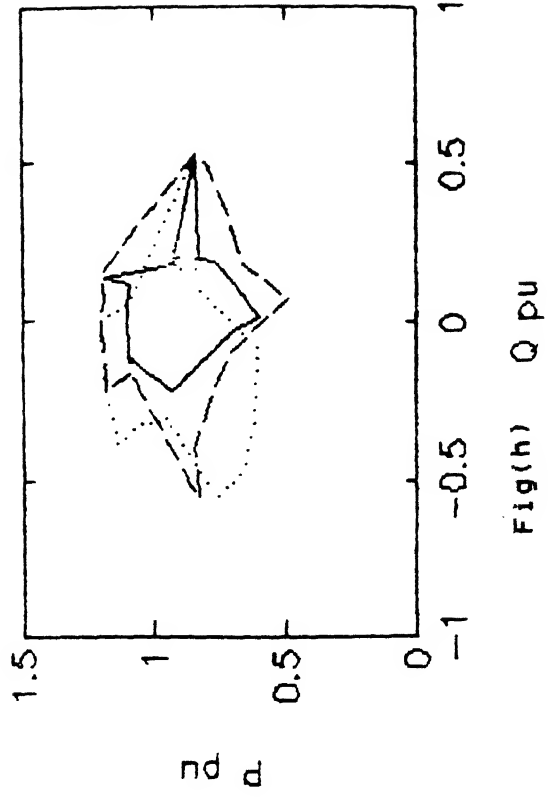
Fig(e) Q pu



Fig(f) Q pu



Fig(g) Q pu



Fig(h) Q pu

Table 3.11 : Numerical Results for Coordinated $\Delta\omega$ Input PSS and ΔP_m Input SVC Stabilizer

Transfer functions of PSS and SVC stabilizer chosen for coordination	Location of closed loop eigenvalues	Range of robustness on 1 p.u. MVA semicircle (P, Q)
PSS	-139.87	
$F_s(s) = \frac{-0.092s^2 - 0.81s - 1.07}{s^2 + 30s + 200}$	- 82.83	(0.824, 0.56)
	- 3.48 ± j12.42	To (0.898, -0.44)
SVC stabilizer	-12.99	
$F_c(s) = \frac{0.271s^2 - 4.086s - 7.23}{s^2 + 24s + 80}$	- 2.01	
	- 4.75	
	-19.36	

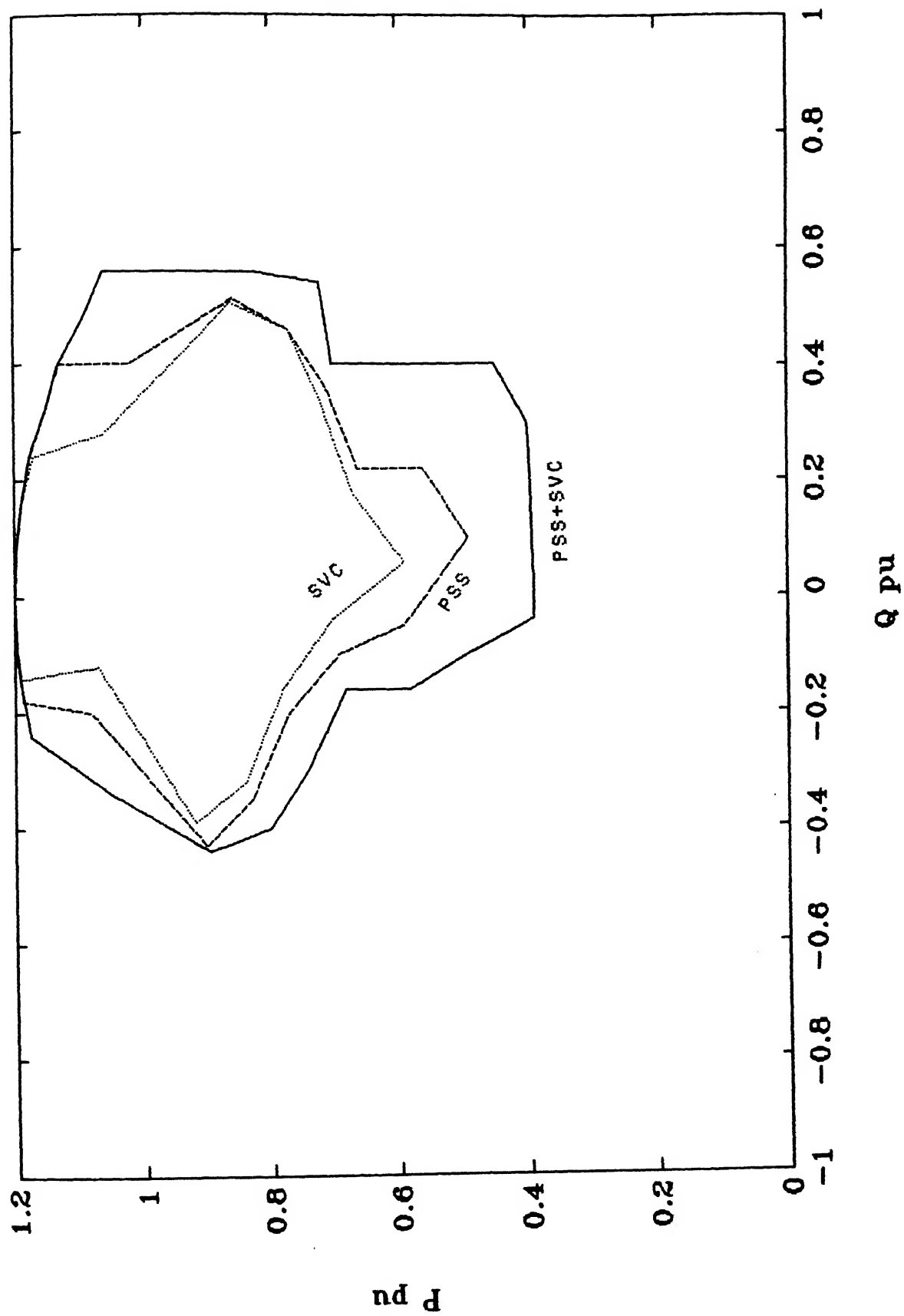


Fig. 3.13 Region of Robustness for $\Delta\omega$ Input PSS and PSS and ΔP_m Input SVC Stabilizer

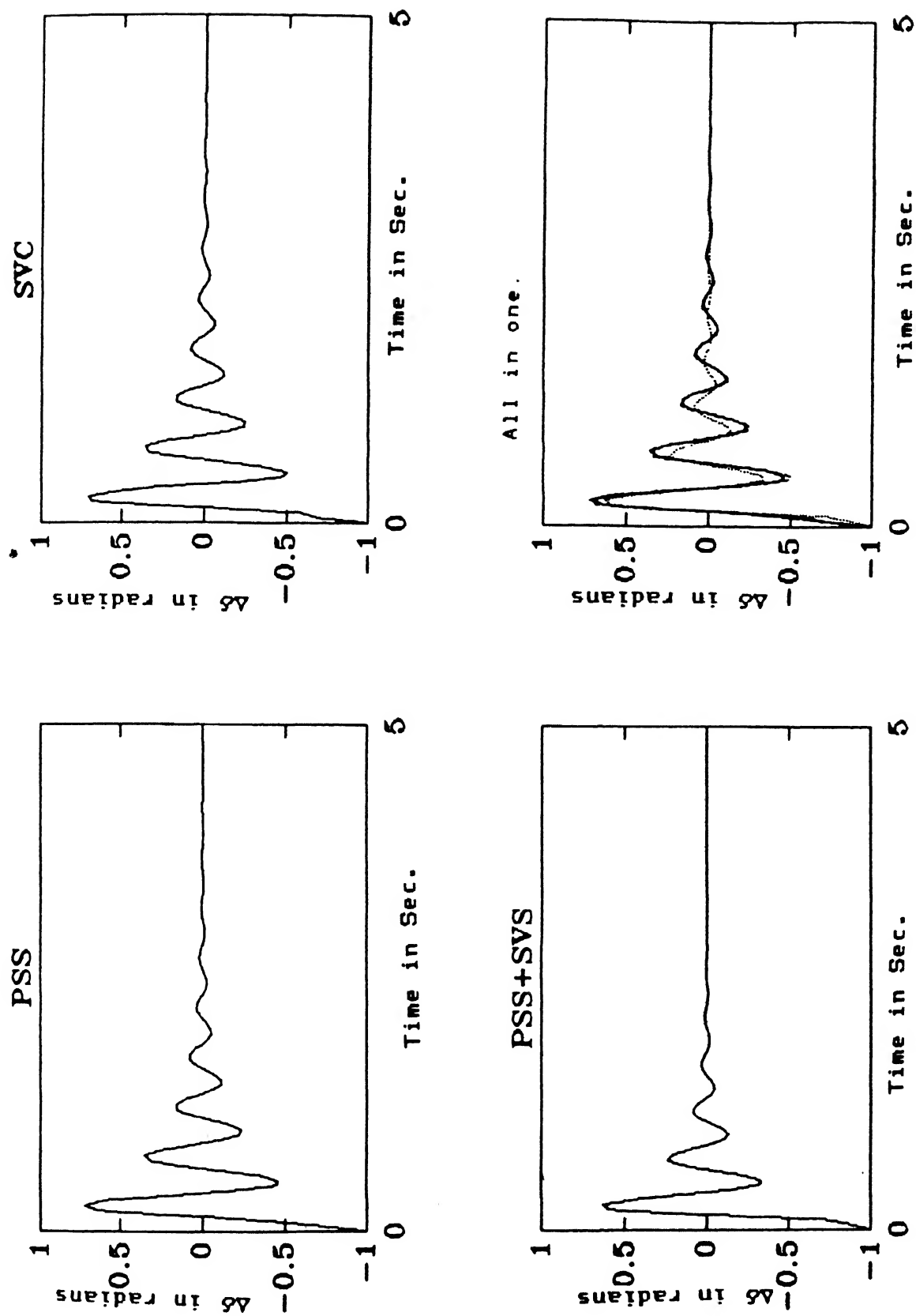
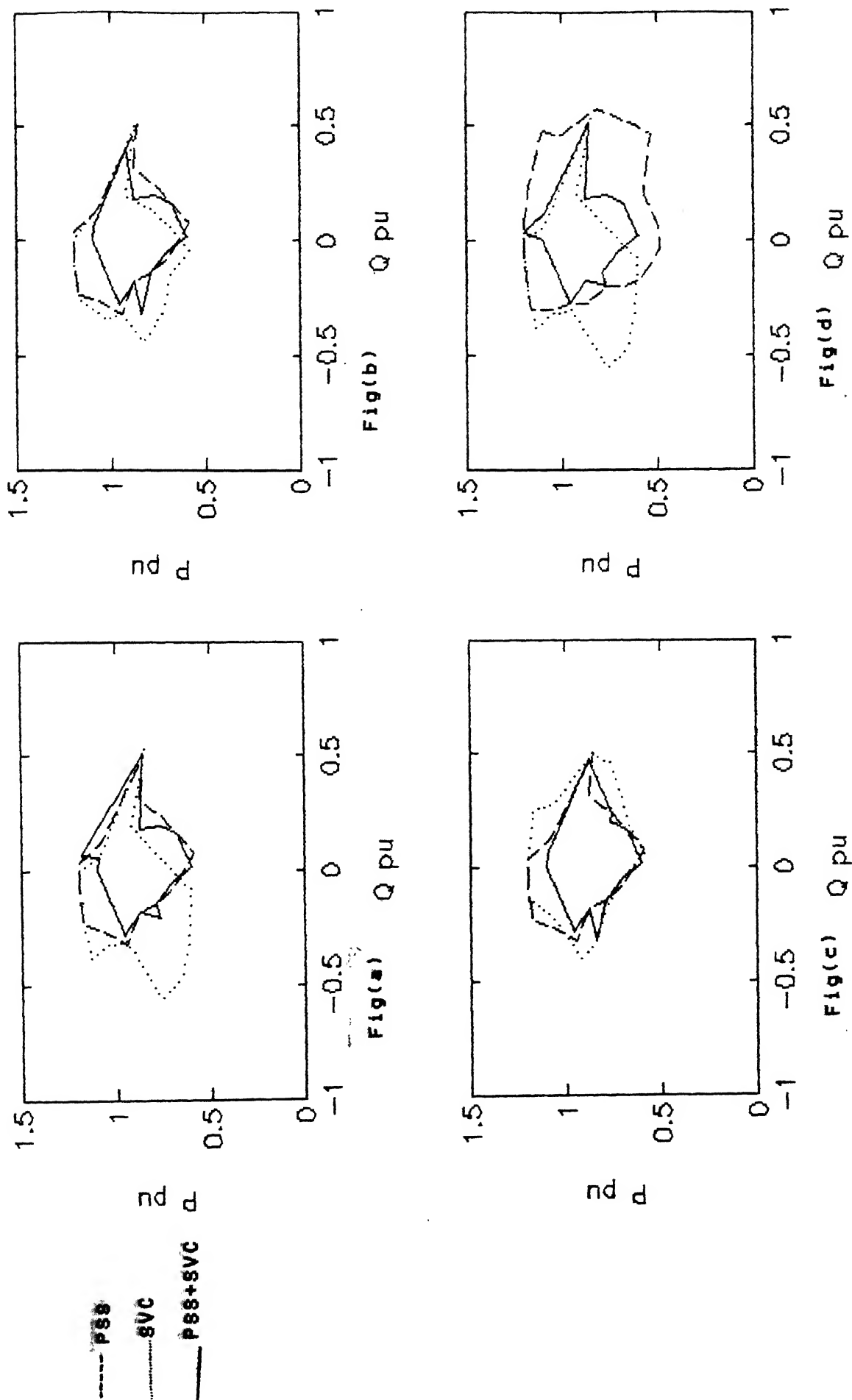


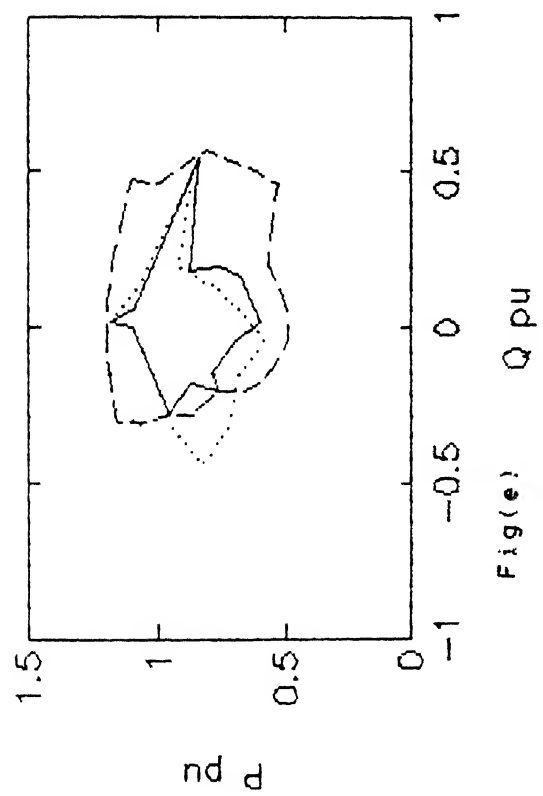
Fig. 3.14 Initial Condition Response of $\Delta\delta$; $\Delta\omega$ Input
PSS and ΔP_m Input SVC Stabilizer

Table 3.12 Numerical Results for Other Pairs of $\Delta\omega$ input P.S.S.
and ΔP_m input S.V.C. Stabilizer not
Selected for Coordination

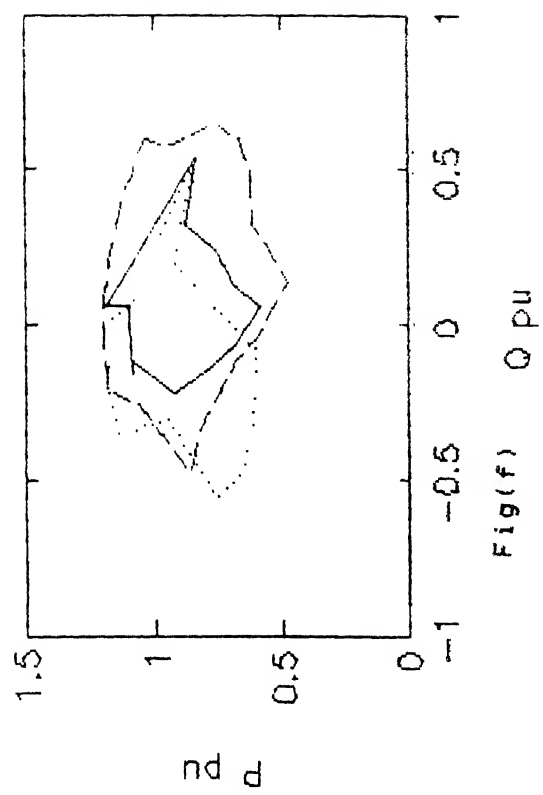
Sl.No of P.S.S. chosen from Table 3.2	Sl.No of S.V.C. Stabilizer chosen from Table 3.3	Range of robustness on 1 p.u. MVA semicircle (P , Q)	Sub-Fig.No. under Fig. No 3.15
1	1	(0.85 , 0.52) to (0.96 , -0.278)	Fig.(a)
1	2	(0.88 , 0.47) to (0.962 , -0.278)	Fig.(b)
1	3	(0.88 , 0.47) to (0.962 , -0.278)	Fig.(c)
2	1	(0.82 , 0.572) to (0.96 , -0.28)	Fig.(d)
2	2	(0.82 , 0.57) to (0.98 , -0.22)	Fig.(e)
2	3	(0.82 , 0.57) to (0.98 , -0.2)	Fig.(f)
3	1	(0.86 , 0.51) to (0.92 , -0.41)	Fig.(g)
3	2	(0.86 , 0.5) to (0.90 , -0.43)	Fig.(h)

Fig. 3.15 Region of Robustness for $\Delta\omega$ Input PSS and ΔP_m Input SVC Stabilizer
 not selected for coordination

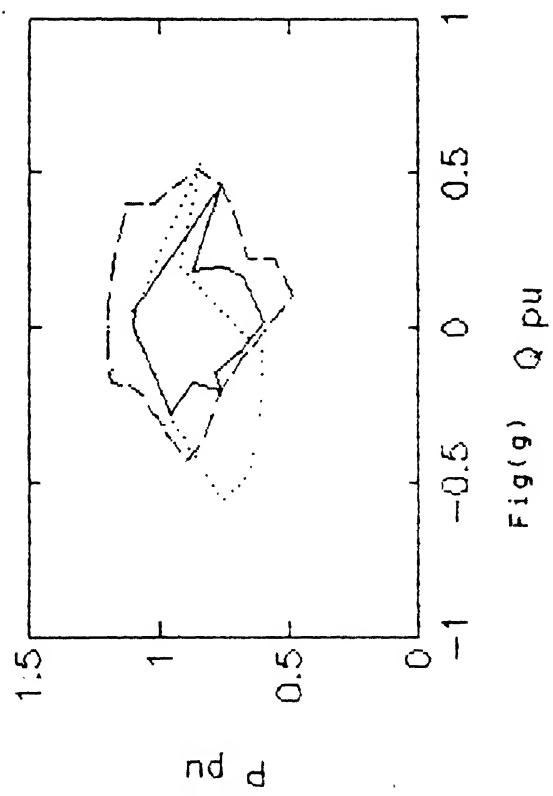




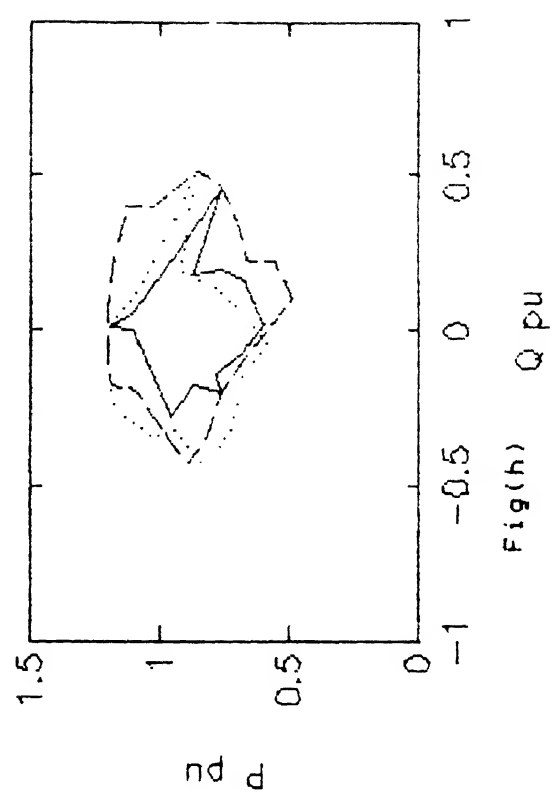
Fig(e)



Fig(f)



Fig(g)



Fig(h)

3.8 A Few Remarks on Design

While determining the region of robustness we have maintained the S.V.C. bus voltage constant at 1.02 p.u. irrespective of the power being transmitted in the line. This can call for a higher capacity of S.V.C. to be installed. But in practice, S.V.C. voltage controller reference setting is made to change depending upon the power flowing through the S.V.C. bus. This is to optimize the rating of S.V.C. to be installed. To simplify our design procedure we have maintained a constant voltage as mentioned above. The validity of our results have to be reestablished for such practical situations where the S.V.C. reference voltage is changed with respect to power flow.

The second remark is on the power factor of the generator, when the S.V.C. is operating at the midpoint of the transmission line with the instruction to maintain certain level of voltage, the generator power factor is mainly decided by the power demand and S.V.C. rating. This is quite an encouraging factor to the results we have presented as it really implies that in practice the stabilizer that we have designed will not encounter most of the operating points in the robustness region at all. Our intention was to highlight the fact that under any operating condition of the generator the scheme that we have proposed can work well.

Finally a few words about the region of robustness. We have tested the robustness range of the stabilizer by changing the MVA output of the generator from 1.2 p.u. MVA to 0.2 p.u. MVA in steps of 0.1 p.u. MVA.

But in practice, the stabilization may not be required when the generator is working at low loads. Dynamic stability problem is usually encountered near full load operation. At low loads even if the low frequency oscillation exists, it is not as serious as at high loads, and it may not lead to the tripping of the transmission lines etc. as the transmission lines are operating far below their rated transmission capacity.

3.0 Concluding Remarks

In this chapter we have designed PSS and SVC stabilizer for a power system. Stabilizers are designed considering power and angular frequency as input signals. Then we have coordinated both the stabilizers by computer aided trial and error method. At the end of this process we have come up with a set of empirical rules to coordinate P.S.S. and S.V.C. stabilizer to give better system performance. Robustness criterion has been chosen to grade the performance of a stabilizer. From the results presented in this chapter, it is also clear that if one of the stabilizers fail to operate, the system is robust enough in the individual robustness range of the stabilizer which is working.

CHAPTER 4

CONCLUSIONS

In this thesis we have shown how P.S.S. and S.V.C. stabilizer designed independently can be coordinated to obtain a further improvement in system performance from dynamic stability point of view.

We have presented a new model of the power system for the dynamic stability analysis of a generator connected to an infinite bus through a transmission line with S.V.C. at the midpoint of the transmission line. The model proposed is simple and straight forward.

P.S.S. and S.V.C. stabilizers are designed independently using pole placement technique. We have then coordinated the P.S.S. and S.V.C. stabilizer by computer aided trial and error method. In all the design and coordination processes robustness was our main concern. At the end of the coordination process we have come up with a set of rules to coordinate P.S.S. and S.V.C. stabilizer in power system.

The coordination process is done considering power and speed signal for P.S.S. and power and angular frequency signal for S.V.C. stabilizer. The results presented clearly indicate that in all the combinations of P.S.S. and S.V.C. that we have chosen for coordination, if one of the stabilizer fails to operate, a minimum region of robustness equal to the individual robustness of the stabilizer that is working is always ensured.

SUGGESTIONS FOR FURTHER WORK

1. We have not fixed the rating of S.V.C. in this thesis. It has been assumed that the S.V.C. has enough capacity to maintain the voltage that we specified at S.V.C. bus. But in practice there is a limit for S.V.C. operation both on inductive and capacitive range, fixed by its rating. Studying the system performance fixing SVC rating is an interesting area to work.
2. We have considered a simple third order generator model, neglecting damper circuit. The results obtained in this thesis may be tested on a higher order generator model taking into account damper windings.
3. We have considered single input stabilizer. Work can be carried out considering two input stabilizers.

REFERENCES

1. Hanson Goodwin and Dandeno, "Influence of Excitation and Speed Control Parameters in Stabilizing Intersystem Oscillations", IEEE Trans. PAS-87, pp. 1306-13, 1968.
2. R.T. Byerly, F.W. Kcay et al., "Damping of Power Oscillations in Salient Pole Machines with Static Exciters", IEEE Trans. Power App. Sys., Vol. PAS-89, pp. 1009-1021, July/Aug. 1970.
3. de Mello and C. Concordia, "Concepts of Synchronous Machine Stability as Affected by Excitation Control", IEEE Trans. PAS, April 1969 pp. 189-201.
4. D.P. Sengupta, "Dynamic Stability in Electric Power Systems", IE(I) Journal El. Special Issue on the state of art in Electrical Engineering, Vol. 70, pp. 117-124, August 1984.
5. E.V. Larsen and D.A. Swann, "Applying Power System Stabilizers", IEEE Trans. on Power Apparatus and Systems, Vol. PAS-100, No. 6, pp. 3017-3046, June 1981.
6. E. Irving, J.P. Barret et al., "Improving Power Network Stability and Unit Stress with Adaptive Generator Control", Automatica, Vol. 15, No. 1, pp. 31-46, January 1979.
7. A. Ghosh, G. Ledwich, O.P. Malik and G.S. Hope, "Power System Stabilizer based on Adaptive Control Techniques", IEEE Trans. on Power Apparatus and Systems, Vol. PAS-103, No. 8, pp. 1983-1989, August 1984.

8. P. Bonanomi, G. Guth, F. Blaser and H. Glavitsch, "Concept of a Practical Adaptive Regulator for Excitation Control", Paper A79453-2, IEEE 1979.
9. Gautam Bandyopadhyay and S.S. Prabhu, "A New Approach to Adaptive Power System Stabilizers", Elect. Mach. and Power System, 1988 pp. 111-125.
10. G.N. Madhu, "Robustness considerations in Adaptive Power System Stabilizer Design", M.Tech. Thesis, Electrical Engineering Department, I.I.T. Kanpur, 1990.
11. Hiromichi Kinoshita, "Improvement of Power System Dynamic Stability by Static Shunt VAR System", Electrical Engineering in Japan, Vol. 99, No. 6, 1979 pp. 81-89.
12. Padiyar, K.R. Rajasekharam, "Dynamic Stabilization of Power System Through reactive Power Modulation", Elec. Mach. & Power Syst. (1986) pp. 281-293.
13. Varma, R.K., "Control of Static VAR Systems for Improvement of Dynamic Stability and Damping of Torsional Oscillations", Ph.D. Thesis, Electrical Engineering Department, I.I.T. Kanpur (April 1988).
14. K. Ramar and A. Srinivas, "Suppression of Low Frequency Oscillations using Static VAR Compensator Controls", Elect. Mach. & Power Systems (1989) pp. 109-123.
15. R.M. Hamouda, M.R. Irvani and Hacham, "Coordinated Static VAR Compensators and Power System Stabilizers for Damping Power System Oscillations", IEEE Trans. Vol. PWRS-2 No.4, November 1987, pp. 1059-1067.

16. C.H. Cheng, Y.Y. Hsu, "Application of Power System Stabilizer and a Static VAR Controller to a Multimachine Power System", IEE Proc. Vol. 137, Jan. 1990 pp. 8-12.
17. Anwaruddin Anwar, "Investigation into Design of Power System Stabilizers", Ph.D. Thesis, Electrical Engineering Department, I.I.T. Kanpur, 1985.
18. P. Kundur, "Practical Experience in Power System Stabilizer Application", Proc. of Workshop on Stabilization Techniques in Power Systems, The Inst. of Engineers (India), December 1986.
19. Heffron W.G. and Phillips, R.A., "Effect of a Modern Amplidyne Voltage Regulator on Under Excited Operation of Large Turbine Generators", AIEE Trans. 1952 pp. 692-697.
20. K.R. Padciyar and R.S. Ramshaw, "A Generalized Synchronous Machine Model for Large Scale Power System Dynamic Studies", Proc. of Seventh PICA Conference, pp. 261-268, Boston, Massachusetts, May 1971.
21. P.M. Anderson and A.A. Fouad, "Power System Control and Stability", Iowa State University Press.
22. IEEE Committee Report "Computer Representation of Excitation Systems", IEEE Trans. PAS, Vol. 87 (June 1968) pp. 1460-1464.
23. N.Munro and S. Novin-Hirbod, "Pole Assignment Using Full-rank Output Feedback Compensators", In. J. Systems.Sci., 1979, Vol. 10, No.3 pp. 285-306.

APPENDIX A

STATE SPACE MODEL OF THE SYSTEM

A.1 Development of the Model

The system model is developed on lines similar to those of [19].

The power system consists of a synchronous generator connected to an infinite bus through a transmission line. Static VAR compensator (SVC) is installed at the midpoint of the transmission line (See. Fig. (2.1)).

The following assumptions are made for developing a state space model of the system.

1. The synchronous machine has no damper windings.
2. Governor and turbine dynamics can be ignored.
3. The machine stator and external network are in quasi-steady state.
4. Magnetic saturation in generator is neglected.

A.1.1 Generator Model

A third order generator model is considered. The equation and notations are standard, see for example, [21]. The equations are given below:

$$pE_q' = -\frac{E_q'}{T_{do}} + \frac{E_{FD}}{T_{do}} + (X_d - X_d') I_d \quad (A.1)$$

$$p\omega = \frac{1}{M} (T_m - T_e) - \frac{K_D}{M} (\omega - \omega_0) \quad (A.2)$$

$$P\delta = \omega - \omega_0 \quad (A.3)$$

where

$$M = \frac{2H}{\omega_0}$$

$$T_e = 3(V_d I_d + V_q I_q)$$

$$\begin{aligned} V_d &= -x_q' I_q \\ V_q &= x_d' I_d + E_q' \end{aligned} \quad (A.4)$$

All quantities are in p.u. except δ and ω , which are in radian and rad/sec respectively.

A.1.2 Excitation System Model

A single time constant excitation system, IEEE Type IS [22] is considered. Fig. (2.2) gives a block diagram representation of the system.

The dynamical equation representing the excitation system is

$$PE_{FD} = -\frac{E_{FD}}{T_A} + \frac{K_A}{T_A} (V_{ref} - V_t + V_{ss}) \quad (A.5)$$

where V_t can be represented in terms of Park's voltages as

$$V_t = (V_d^2 + V_q^2)^{1/2}$$

where

$$\begin{aligned} V_d &= -x_q' I_q \\ V_q &= x_d' I_d + E_q' \end{aligned}$$

A.1.3 SVC Model

A single time constant SVC voltage controller is considered. The block diagram representation of SVC voltage controller is given in Fig. (2.3).

The dynamical equation representing SVC voltage controller is

$$PB = - \frac{B}{T_B} + \frac{K_B}{T_B} (V_{mref} - V_m + V_{se}) \quad (A.6)$$

A.1.4 Linearized Model

The linearized state space model is derived by linearizing eqns. (A.1), (A.2), (A.3), (A.5) and (A.6). The non state variables ΔI_d , ΔT_e , ΔV_t and ΔV_m are represented in terms of state variables as follows.

A.1.4.1 Expressions for ΔI_d and ΔI_q

To obtain expressions for ΔI_d and ΔI_q in terms of state variables the system in Fig. (2.1) is reduced to the form shown in Fig. (A.1) by star-delta transformation. The impedance then reflecting between the infinite bus and the ground can be neglected.

For the system in Fig. A.1, we can write the following equations as in [21], Sec. 5.4,

$$V_d (1+\lambda_1) + V_q \lambda_2 = - V_\omega \sin(\delta-\alpha) + R_e I_d + x_e I_q \quad (A.7)$$

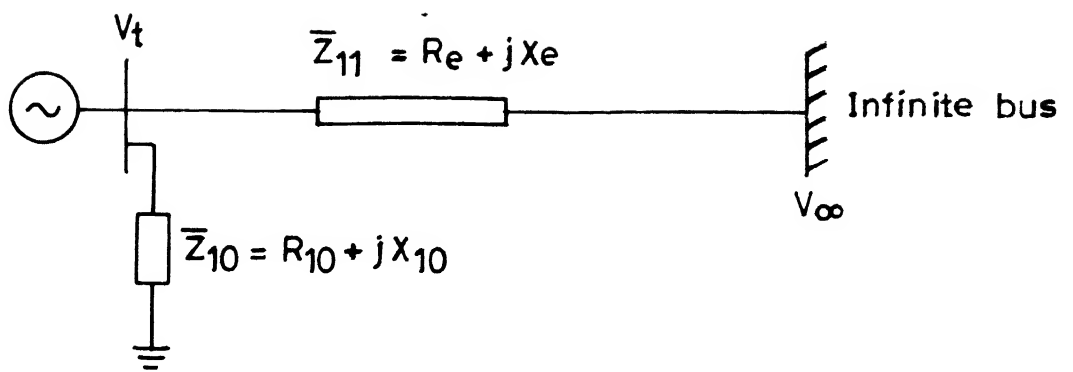


Figure A1 Equivalent circuit of the system.

$$-V_d \lambda_2 + V_q (1 + \lambda_1) = V_\omega \cos(\delta - \alpha) - x_e I_d + R_e I_q \quad (A.8)$$

where α and δ are as defined in [21], Sec. 5.4,

$$\begin{aligned} R_{10} &= R & R_e &= 2R - 2XB \\ X_{10} &= \left(X - \frac{Z}{B}\right) & X_e &= R^2 B - X^2 B + 2X \\ Z_{10}^2 &= R^2 + \left(X - \frac{Z}{B}\right)^2 \\ \lambda_1 &= \frac{(R_{10} R_e + X_{10} X_e)}{Z_{10}^2}, \lambda_2 = \frac{R_{10} X_e - X_{10} R_e}{Z_{10}^2} \end{aligned} \quad (A.9)$$

Linearizing equation (A.7) and (A.8) we obtain expression for ΔI_d and ΔI_q in terms of state variables as

$$\begin{bmatrix} \Delta I_d \\ \Delta I_q \end{bmatrix} = \begin{bmatrix} b_{11} & b_{12} & b_{13} \\ b_{21} & b_{22} & b_{23} \end{bmatrix} \begin{bmatrix} \Delta E_q' \\ \Delta \delta \\ \Delta B \end{bmatrix} \quad (A.10)$$

where

$$b_{11} = - \left[\frac{b_5 B_0 - b_2 (1 - B_0 X)}{b_1 b_5 - b_2 b_4} \right] \quad (A.11)$$

$$b_{12} = - \left[\frac{b_5 V_\omega \cos(\delta_0 - \alpha) - b_2 V_\omega \sin(\delta_0 - \alpha)}{b_1 b_5 - b_2 b_4} \right] \quad (A.12)$$

$$b_{13} = \left[\frac{b_3 b_5 - b_2 b_6}{b_1 b_5 - b_2 b_4} \right] \quad (\text{A.13})$$

$$b_{21} = - \left[\frac{b_4 B_o - b_1 (1 - B_o X)}{b_2 b_4 - b_1 b_5} \right] \quad (\text{A.14})$$

$$b_{22} = - \left[\frac{b_4 V_\infty \cos(\delta_o - \alpha) - b_1 V_\infty \sin(\delta_o - \alpha)}{b_2 b_4 - b_1 b_5} \right] \quad (\text{A.15})$$

$$b_{23} = \left[\frac{b_3 b_4 - b_1 b_6}{b_2 b_4 - b_1 b_5} \right] \quad (\text{A.16})$$

In the above equations

$$b_1 = B_o \dot{X}_d R - 2R + 2B_o RX$$

$$b_2 = -X_q + B_o X_q X - R^2 B_o + X^2 B_o - 2X$$

$$b_3 = - \left[I_{qo} X_q X + I_{do} \dot{X}_d R + E_{qo} R + 2I_{do} RX - I_{qo} R^2 + I_{qo} X^2 \right]$$

$$b_4 = \left[\dot{X}_d - \dot{X}_d X B_o + R^2 B_o - X^2 B_o + 2X \right]$$

$$b_5 = \left[X_q R B_o - 2R + 2RX B_o \right]$$

$$b_6 = - \left[X_q R I_{qo} - \dot{X}_d X I_{do} - X E_{qo} + R^2 I_{do} - X^2 I_{do} + 2RX I_{qo} \right]$$

(A.17)

A.1.4.2 Expressions for ΔT_e

$$T_e = 3 (V_d I_d + V_q I_q) \text{ p.u.}$$

where

$$V_d = - X_q I_q$$

$$V_q = X_d' I_d + E_q'$$

$$\text{Therefore } T_e = 3 \left[E_q' I_q - (X_q - X_d') I_d I_q \right] \quad (\text{A.18})$$

Linearizing equation (A.18) and then substituting for ΔI_d and ΔI_q from equation (A.10) we get

$$\Delta T_e = M \left[b_{40} \Delta E_q' + b_{42} \Delta \delta + b_{43} \Delta B \right] \quad (\text{A.19})$$

where

$$b_{40} = 3 \left[b_{21} (E_{q0}' - X_q I_{d0} + X_d' I_{d0}) + b_{11} (I_{q0} X_d' - I_{q0} X_q) + I_{q0} \right]$$

$$b_{42} = 3 \left[b_{22} (E_{q0}' - X_q I_{d0} + X_d' I_{d0}) + b_{12} (I_{q0} X_d' - I_{q0} X_q) \right]$$

$$b_{43} = 3 \left[b_{23} (E_{q0}' - X_q I_{d0} + X_d' I_{d0}) + b_{13} (I_{q0} X_d' - I_{q0} X_q) \right]$$

(A.20)

A.1.4.3 Expression for ΔV_t

For generator terminal voltage V_t we can write

$$V_t^2 = V_d^2 + V_q^2 \quad (\text{A.21})$$

Linearizing above equation and substituting for ΔI_d and ΔI_q from equation (A.10) we can write

$$\Delta V_t = K_6 \Delta E_q' + K_5 \Delta \delta + K_9 \Delta B \quad (\text{A.22})$$

where

$$\begin{aligned} K_6 &= - \frac{V_{d0}}{V_{t0}} X_q b_{21} + \frac{V_{q0}}{V_{t0}} X_d' b_{11} + \frac{V_{q0}}{V_{t0}} \\ K_5 &= - \frac{V_{d0}}{V_{t0}} X_q b_{22} + \frac{V_{q0}}{V_{t0}} X_d' b_{12} \\ K_9 &= - \frac{V_{d0}}{V_{t0}} X_q b_{23} + \frac{V_{q0}}{V_{t0}} X_d' b_{13} \end{aligned} \quad (\text{A.22})$$

A.1.4.4 Expression for ΔV_m

For SVC bus voltage V_m we can write

$$V_m^2 = V_{mq}^2 + V_{md}^2 \quad (\text{A.23})$$

where

$$\begin{aligned} V_{md} &= V_d - I_d R - I_q X \\ V_{mq} &= V_q - I_q R + I_d X \end{aligned}$$

Linearizing equation (A.23) and substituting for ΔI_q and ΔI_d from (A.10) we get

$$\Delta V_m = b_{56} \Delta E_q' + b_{57} \Delta \delta + b_{58} \Delta B \quad (\text{A.24})$$

The final state equations are obtained after substituting for ΔI_d , ΔT_e , ΔV_t and ΔV_m in terms of state variables, in eqns. (A.1), (A.2), (A.3), (A.5) and (A.6). The resulting fifth order system state equation can be written as

$$\dot{\underline{x}} = A \underline{x} + \underline{b}_1 u_1 + \underline{b}_2 u_2 \quad (\text{A.25})$$

where

$$\dot{\underline{x}} = \left[\Delta E_q' \quad \Delta \omega \quad \Delta \delta \quad \Delta E_{FD} \quad \Delta B \right]^t \quad (\text{A.26})$$

and $u_1 = \Delta V_{ss}$, stabilizing signal from PSS

$u_2 = \Delta V_{se}$, stabilizing signal from SVC stabilizer

(A.27)

A_1 , b_1 and b_2 matrices are given as

$$A = \begin{bmatrix} A_{11} & 0 & A_{13} & A_{14} & A_{15} \\ A_{21} & A_{22} & A_{23} & 0 & A_{25} \\ 0 & A_{32} & 0 & 0 & 0 \\ A_{41} & 0 & A_{43} & A_{44} & A_{45} \\ A_{51} & 0 & A_{53} & 0 & A_{55} \end{bmatrix} \quad (\text{A.28})$$

$$\underline{b}_1 = \left[0 \quad 0 \quad 0 \quad b_4 \quad 0 \right]^t \quad (\text{A.29})$$

$$\underline{b}_2 = \left[0 \quad 0 \quad 0 \quad 0 \quad b_5 \right]^5 \quad (\text{A.30})$$

where

$$A_{11} = \frac{[(X_d - X_d') b_{11} - 1]}{T_{do}}$$

$$A_{13} = \frac{(X_d - \dot{X}_d) b_{12}}{\dot{T}_{do}}$$

$$A_{14} = \frac{(X_d - \dot{X}_d) b_{13}}{\dot{T}_{do}}$$

$$A_{15} = \frac{1}{\dot{T}_{do}}$$

$$A_{21} = 3 \left[b_{21} (\dot{E}_{q0} - X_q I_{do} + \dot{X}_{do} I_{do}) + b_{11} (\dot{X}_d I_{q0} - X_q I_{q0}) + I_{q0} \right]$$

$$A_{23} = 3 \left[b_{22} (\dot{E}_{q0} - X_q I_{do} + \dot{X}_{do} I_{do}) + b_{12} (\dot{X}_d I_{q0} - X_q I_{q0}) \right]$$

$$A_{25} = 3 \left[b_{23} (\dot{E}_{q0} - X_q I_{do} + \dot{X}_{do} I_{do}) + b_{13} (\dot{X}_d I_{q0} - X_q I_{q0}) \right]$$

$$A_{22} = - \frac{K_D}{M}$$

$$A_{32} = 1$$

$$A_{41} = - \frac{K_6 K_A}{T_A}$$

$$A_{43} = - \frac{K_5 K_A}{T_A}$$

$$A_{44} = - \frac{1}{T_A}$$

$$A_{45} = - \frac{K_9 K_A}{T_A}$$

$$A_{51} = - \frac{K_B b_{56}}{T_B}$$

$$A_{53} = - \frac{K_B b_{57}}{T_B}$$

$$A_{55} = - \frac{1 + K_B b_{58}}{T_B}$$

$$\begin{aligned}
b_4 &= \frac{K_A}{T_A} \\
b_5 &= \frac{K_B}{T_B}
\end{aligned}
\tag{A.31}$$

A.1.5 Output Equations

The output equation of the system can be written as

$$y_1 = c_1 \underline{x}$$

where y_1 represents input to PSS, and

$$y_2 = c_2 \underline{x}$$

where y_2 represents input to SVC stabilizer.

The elements of matrices c_1 and c_2 depend upon the particular variables chosen as y_1 and y_2 .

A.1.5.1 Output Equations Corresponding to PSS Signals

For PSS we have considered rotor speed and generator accelerating power as control signals.

Speed Signal

Change in rotor speed ($\Delta\omega$) is utilized as control signal. Since speed is one of the state variables in our system model, the output equation is directly obtained as

$$y_1 = [\Delta\omega] = \begin{bmatrix} 0 & 1 & 0 & 0 & 0 \end{bmatrix} \underline{x} \tag{A.32}$$

$$\text{Thus, } c_2 = \begin{bmatrix} 0 & 1 & 0 & 0 & 0 \end{bmatrix} \tag{A.33}$$

Power Signal

Generator power output is taken as control signal. When expressed in p.u. $\Delta P_e = \Delta T_e$. Hence we can write the output equation corresponding to power signal as

$$y_1 = \begin{bmatrix} \Delta P_e \end{bmatrix} = \begin{bmatrix} b_{40} & 0 & b_{41} & 0 & b_{42} \end{bmatrix} x \quad (\text{A.34})$$

Thus,

$$c_1 = \begin{bmatrix} b_{40} & 0 & b_{41} & 0 & b_{42} \end{bmatrix} \quad (\text{A.35})$$

where $b_{40} \dots b_{42}$ are as given in the expression for ΔT_e , (eqn. (A.19) and (A.20)).

A.1.5.2 Output Equations Corresponding to SVC Stabilizer Signals

For SVC stabilizer we have considered midline power and SVC bus angular frequency signals.

Midline Power Signal:

The midline power is given by

$$P_m = 3 \left[V_{md} I_d + V_{mq} I_q \right] \quad (\text{A.36})$$

Linearizing the above expression and manipulating we get

$$\Delta P_m = b_{60} \Delta E'_q + b_{61} \Delta \delta + b_{62} \Delta B \quad (\text{A.37})$$

$$\text{where } c_2 = \begin{bmatrix} b_{60} & 0 & b_{61} & 0 & b_{62} \end{bmatrix} \quad (\text{A.38})$$

where

$$b_{60} = b_{11} V_{mdo} + b_{50} I_{do} + b_{21} V_{mqo} + b_{53} I_{qo}$$

$$b_{61} = b_{12} V_{mdo} + b_{51} I_{do} + b_{22} V_{mqo} + b_{54} I_{qo}$$

$$b_{62} = b_{13} V_{mdo} + b_{52} I_{do} + b_{23} V_{mqo} + b_{55} I_{qo} \quad (A.39)$$

In the above equation

$$b_{51} = \left[(-X_q - X) b_{21} - R b_{11} \right]$$

$$b_{52} = \left[(-X_q - X) b_{22} - R b_{12} \right]$$

$$b_{53} = \left[(-X_q - X) b_{23} - R b_{13} \right]$$

$$b_{54} = \left[(-R b_{21} + (X + X_d^{\bullet}) b_{11} + 1) \right]$$

$$b_{55} = \left[(-R b_{22} + (X + X_d^{\bullet}) b_{12} \right]$$

$$b_{56} = \left[(-R b_{23} + (X + X_d^{\bullet}) b_{13} \right] \quad (A.40)$$

SVC Bus Angular Frequency Signal:

For SVC bus angular frequency ω_s we can write

$$\omega_s = \frac{d}{dt} \left[\tan^{-1} \frac{V_{md}}{V_{mq}} \right]$$

Linearizing the above expression,

$$\Delta \omega_s = \frac{V_{mdo}}{V_{mo}^2} (p \Delta V_{mq}) - \frac{V_{mqo}}{V_{mo}^2} (p \Delta V_{md}) \quad (A.41)$$

we know that

$$V_m = V_{mq} + j V_{md}$$

or

$$V_m^2 = V_{mq}^2 + V_{md}^2 \quad (A.42)$$

Linearizing (A.42),

$$\Delta V_m = \left[\frac{V_{mdo}}{V_{mo}} \right] \Delta V_{md} + \left[\frac{V_{mqo}}{V_{mo}} \right] \Delta V_{mq}$$

Also we can write

$$\left. \begin{aligned} V_{md} &= V_d - I_d R - I_q X \\ V_{mq} &= V_q - I_q R + I_d X \end{aligned} \right\} \quad (A.43)$$

In terms of incremental quantities, we get

$$\left. \begin{aligned} \Delta V_{md} &= b_{50} \Delta E_q + b_{51} \Delta \delta + b_{52} \Delta B \\ \Delta V_{mq} &= b_{53} \Delta E_q + b_{54} \Delta \delta + b_{55} \Delta B \end{aligned} \right\} \quad (A.44)$$

Substituting eqns (A.43) appropriately in eqn. (A.41) we get the final expression for $\Delta \omega_s$ as

$$y_2 = [\Delta \omega_s] = \begin{bmatrix} b_{80} & b_{27} & b_{81} & b_{32} & b_{83} \end{bmatrix} x + \frac{b_{28} K_B}{T_B} \Delta V_{se} \quad (A.45)$$

Thus,

$$c_2 = \begin{bmatrix} b_{80} & b_{27} & b_{81} & b_{82} & b_{83} \end{bmatrix} \quad (A.46)$$

$$d_2 = \frac{b_{28}}{T_B} K_B \quad (A.47)$$

where

$$b_{80} = b_{35} b_{26} - \frac{K_B}{T_B} b_{56} b_{28}$$

$$b_{81} = b_{36} b_{26} - \frac{K_B}{T_B} b_{57} b_{28}$$

$$b_{82} = b_{26} b_{37}$$

$$b_{83} = b_{26} b_{36} - \frac{b_{28}}{T_B} - \frac{K_B b_{28} b_{58}}{T_B} \quad (A.48)$$

Also, $b_{35} = A_{11}$, $b_{36} = A_{13}$, $b_{37} = A_{14}$, $b_{38} = A_{15}$

$$b_{26} = \frac{V_{mdo}}{V_{mo}^2} b_{53} - \frac{V_{mqo}}{V_{mo}^2} b_{50}$$

$$b_{27} = \frac{v_{m d o}}{\sqrt{2}_{m o}} b_{54} - \frac{v_{m q o}}{\sqrt{2}_{m o}} b_{51}$$

$$b_{28} = \frac{v_{m d o}}{\sqrt{2}_{m o}} b_{55} - \frac{v_{m q o}}{\sqrt{2}_{m o}} b_{52} . \quad (A.49)$$

APPENDIX B

POWER SYSTEM DATA

Most of the data are as in [11]. All quantities are expressed in p.u. on a 500 KV, 5000 MVA base.

1. Generator

$$\begin{array}{lll} X_d = 1.7 & X_q = 1.64 & X_d' = 0.345 \\ T_{do}' = 6.4 & H = 4.2 & \omega_0 = 314 \end{array}$$

2. Excitation System

$$K_A = 50 \qquad T_A = 0.01 \text{ sec.}$$

3. SVC Voltage Controller

$$K_B = 20 \qquad T_B = 0.02 \text{ sec.}$$

4. Network Parameters

- i) Step up transformer $x_t = 0.15$
- ii) Transmission (500 KV, 100 km, line constants per circuit)
 - $r_{\text{line}} = 0.0135$
 - $x_{\text{line}} = 0.452$
 - $B_{\text{line}} = 0.02294$

5. Infinite bus voltage: $1.0 \angle 0$ p.u.

6. $K_D = 0.$

APPENDIX C

POLE ASSIGNMENT WITH OUTPUT FEEDBACK [23]

The technique given here is based on the work of Munro and Hirbod [36]. The method presented in [23] provides a technique for the design of full rank compensators for multi variable linear systems. Here the technique is restricted to single input linear systems. We have,

$$\dot{\underline{x}} = \underline{A} \underline{x} + \underline{b} u \quad (\text{C.1})$$

and

$$\underline{y} = \underline{C} \underline{x} \quad (\text{C.2})$$

where, $\underline{x} \in R^n$, $\underline{u} \in R^p$ and $\underline{y} \in R^r$ are respectively vectors of state, input and output variables. The $r \times p$ open loop transfer function matrix $G(s)$ is given by,

$$G(s) = \underline{C}(sI - \underline{A})^{-1} \underline{b} = [1/\mu_0(s)] \begin{bmatrix} N_1(s) \\ \vdots \\ N_r(s) \end{bmatrix} \quad (\text{C.3})$$

where

$$\mu_0(s) = s^n + \alpha_1 s^{n-1} + \dots + \alpha_n \quad (\text{C.4})$$

and

$$N_i(s) = \beta_{i1} s^{n-1} + \beta_{i2} s^{n-2} + \dots + \beta_{in} \quad (\text{C.5})$$

$\mu_0(s)$ is the characteristic polynomial of $G(s)$. Consider output feedback law

$$u(s) = u_r(s) - H(s) \cdot Y(s)$$

where $u_r \in R^p$ represents the reference input.

The problem can be defined as the determination of $p \times r$ dynamic feedback compensator $H(s)$, such that the closed loop system,

$$H(s) = [1 + G(s) H(s)]^{-1} G(s) \quad (C.7)$$

has a desired set of eigenvalues. The k^{th} order compensator $H(s)$ has the form

$$H(s) = [1/\mu_0(s)] [M_1(s), M_2(s) \dots M_r(s)] \quad (C.8)$$

where

$$\mu_c(s) = s^k + \gamma_1 s^{k-1} + \gamma_2 s^{k-2} + \dots + \gamma_k \quad (C.9)$$

and

$$M_i(s) = \theta_{i0} s^k + \theta_{i1} s^{k-1} + \dots + \theta_{ik} \quad (C.10)$$

$\mu_c(s)$ is the characteristic polynomial of compensator transfer function $H(s)$.

The resulting closed loop system characteristic polynomial $\mu_d(s)$, defined as:

$$\mu_d(s) = s^{n+k} + d_1 s^{n+k-1} + \dots + d_{n+k} \quad (C.11)$$

can be written as [23]

$$\mu_d(s) = \mu_0(s) \cdot \mu_c(s) + \sum_{i=1}^r N_i(s) \cdot M_i(s) \quad (C.12)$$

Complete Pole Placement

The problem of pole assignment can be defined as given $\mu_0(s)$, $N_1(s)$, ... $N_r(s)$ and a desired set of closed loop poles, find $\mu_c(s)$, $M_1(s)$, ..., $M_r(s)$ of lowest degree which satisfy eqn.

(C.12). Equating coefficients of like powers of s in eqn.

(C.12), we get

$$[X_k] \cdot \underline{P}_k = \underline{\delta}_k \quad (C.13)$$

where

$$[X_k] = \begin{bmatrix} 1 & 0 & \dots & 0 & \beta_{p1} & \dots & 0 & \beta_{r1} & \dots & 0 \\ \alpha_1 & 1 & \dots & 0 & \beta_{p2} & \dots & 0 & \beta_{r2} & \dots & 0 \\ \alpha_3 & \alpha_2 & & 1 & & & \beta_{p1} & & & \beta_{r1} \\ \cdot & \cdot & & \alpha_1 & \beta_{pn} & & \beta_{p2} & \beta_{rn} & & \beta_{r2} \\ \alpha_n & \cdot & & \alpha_2 & 0 & & & 0 & & \\ 0 & \alpha_n & & & 0 & & & 0 & & \\ \cdot & & & & & & & & & \\ \cdot & & & & & & & & & \\ 0 & 0 & & \alpha_n & 0 & & \beta_{pn} & 0 & & \beta_{rn} \end{bmatrix}$$

$$\underline{P}_k = [\gamma_1 \gamma_2 \dots \gamma_k \mid \theta_{p0} \dots \theta_{pk} \mid \dots \mid \theta_{r0} \dots \theta_{rk}]^t$$

and

$$\underline{\delta}_k = [(d_1 - \alpha_1) \mid (d_2 - \alpha_2) \mid \dots \mid (d_n - \alpha_n) \mid d_{n+1} \dots d_{n+k}]^t$$

Equation (C.13) is a set of $(n+k)$ equations in $[(k+p)r+k]$ unknown parameters of $H(s)$. The difference vector $\underline{\delta}_k$ contains the coefficients of the polynomial

$$\mu_d(s) = \mu_s(s) - \mu_0(s) \cdot s^k \quad (C.14)$$

A necessary and sufficient condition for the existence of solution of eqn. (C.13) is

$$\text{Rank } [X_k] = \text{Rank } [X_k, \delta_k] \quad (\text{C.15})$$

and a solution of eqn. (C.13) is

$$P_{-k} = [X_k^{g1}] \delta_{-k} \quad (\text{C.16})$$

where X_k^{g1} is the generalized inverse of X_k such that

$$[X_k] [X_k^{g1}] [X_k] = [X_k]$$

Partial Pole Placement

Consider the case when only q poles are to be assigned, $t = (n+k-q)$ poles are allowed to assume arbitrary locations. For this case the closed loop systema characteristic polynomial $\mu_d(s)$ has the form

$$\mu_d(s) = (s^q + d_1 s^{q-1} + \dots + d_q)(s^2 + e_1 s^{t-1} + \dots + e_t) \quad (\text{C.17})$$

where d_1, d_2, \dots, d_q are specified and e_1, e_2, \dots, e_t are to be determined. Here the difference vector δ_{-k} can be obtained by equating the coefficients of like powers of s in eqn. (C.17) and (C.12) as

$$\delta_{-k} = \delta_{-k}^* + e_1 \delta_{-1} + \dots + e_t \delta_{-t} \quad (\text{C.18})$$

where the vectors δ_{-k}^* and δ_{-i} , ($i = 1, \dots, t$) contain respectively the coefficients of the polynomials

$$\mu_d''(s) = \mu_q(s) \cdot s^t - \mu_0(s) \cdot s^k \quad (\text{C.19})$$

$$\mu_i''(s) = \mu_q(s) \cdot s^{t-1}, \quad (i = 1, \dots, t) \quad (C.20)$$

Eqn. (C.13) in this case will take the form

$$[X_k] \underline{P}_k = \delta_k^* + [D] \underline{e} \quad (C.21)$$

where

$$[D] = [\delta_1, \delta_2, \dots, \delta_t]$$

and

$$\underline{e} = [e_1, e_2, \dots, e_t]^t$$

Eqn. (C.21) can be rearranged as

$$[X_k^*] \underline{P}_k^* = \delta_k^* \quad (C.22)$$

where

$$[X_k^*] = [X_k, -D]$$

and

$$\underline{P}_k^* = [\underline{P}_k^t, \underline{e}^t]^t \quad (C.23)$$

Eqn. (C.22) is a set of $(n+k)$ simultaneous algebraic equations in $[r(k+p) + k+t]$ unknowns. Vector \underline{P}_k^* contains parameters of $H(s)$ and the coefficients of polynomial of unassigned closed loop poles. The necessary and sufficient condition for the existence of solution of eqn. (C.22) is given in eqn. (C.15) with \underline{X}_k , \underline{P}_k and δ_k replaced by \underline{X}_k^* , \underline{P}_k^* and δ_k^* respectively.